Mechanical System Lifetime

Raed Kouta, Sophie Collong, and Daniel Play

Abstract We present, in three parts, the approaches for the random loading analysis in order to complete methods of lifetime calculation.

First part is about the analysis methods. Second part considers modeling of random loadings. A loading, or the combination of several loadings, is known as the leading cause of the dwindling of the mechanical component strength. Third part will deal with the methods taking into account the consequences of a random loading on lifetime of a mechanical component.

The motivations of the present document are based on the observation that operating too many simplifications on a random loading lost much of its content and, therefore, may lose the right information from the actual conditions of use. The analysis of a random loading occurs in several ways and in several approaches, with the aim of later evaluate the uncertain nature of the lifetime of a mechanical component.

Statistical analysis and frequency analysis are two complementary approaches. Statistical analyses have the advantage of leading to probabilistic models (Demoulin B (1990a) Processus aléatoires [R 210]. Base documentaire « Mesures. Généralités ». (*)) provide opportunities for modeling the natural dispersion of studied loadings and their consequences (cracking, fatigue, damage, lifetime, etc.). The disadvantage of these statistical analyses is that they ignore the history of events.

On the other hand, the frequency analyses try to remedy this drawback, using connections between, firstly, the frequencies contained in the loading under consideration and, secondly, whether the measured average amplitudes (studied with

R. Kouta (✉) • S. Collong
University of Technology of Belfort-Montbéliard, 90010 Belfort Cedex, France
e-mail: raed.kouta@utbm.fr

D. Play
INSA of Lyon, 69621 Villeurbanne Cedex, France

S. Kadry and A. El Hami (eds.), *Numerical Methods for Reliability and Safety Assessment: Multiscale and Multiphysics Systems*, DOI 10.1007/978-3-319-07167-1_1,

the Fourier transform, FT) or their dispersions (studied with the power spectral density, PSD) (Kunt M (1981) Traitement numérique des signaux. Éditions Dunod; Demoulin B (1990b) Fonctions aléatoires [R 220]. Base documentaire « Mesures. Généralités ». (*)). The disadvantage of frequency analyses is the need to issue a lot of assumptions and simplifications for use in models of lifetime calculation (e.g., limited to a system with one degree of freedom using probabilistic models simplified for the envelope of the loading).

A combination of the two analyses is possible and allows a good fit between the two approaches. This combination requires a visual interpretation of the appearance frequency. Thus, a random loading is considered a random process to be studied at the level of the amplitude of the signal, its speed, and its acceleration.

1 Random Loadings Analysis

1.1 Usual Conditions of a Mechanical System

Mechanical systems and mechanical components provide functions for action more or less complicated. These actions are performed and controlled by one or more users in a variety of conditions (Schütz 1989). The diversity of uses leads to a large number of load situations. The challenge for designers of mechanical systems and mechanical components integrates these actual conditions of use (Heuler and Klätschke 2005). More generally, the challenge is to take into account the possibly nondeclared or explicit wishes of the users. Practically, it is to consider the diversity of loads and stresses applied to mechanical components. This condition is added to the geometric optimization requirements and conditions of material strength (Pluvinage and Sapunov 2006). It requires the development of a calculation tool suitable for both to obtain a representative model of loads and to carry out design calculations (Weber 1999).

Taking into account the actual conditions of use become a technological and economic challenge. But it causes a profound change in attitude since the causes are considered a probable way from assumptions used by a significant segment of the population. And of course, the calculation of the effects will be presented in terms of probability of strength and reliability (Lannoy 2004). This approach is possible because the two parts of the modeling are now well understood. Firstly, the effects of various loads applied to the components can be analyzed and calculated in terms of dynamic loads (Savard 2004; Bedard 2000). Then, the physical behavior of materials subjected to repeated stress is better known (Lu 2002; Rabbe and Galtier 2000). The design engineer can then develop methods for calculations reconciling best current knowledge and objectives he must achieve. Upstream of the approach, the loads from the conditions imposed by the users must be known. And downstream of the approach, it is necessary to calculate the consequences of such loads.

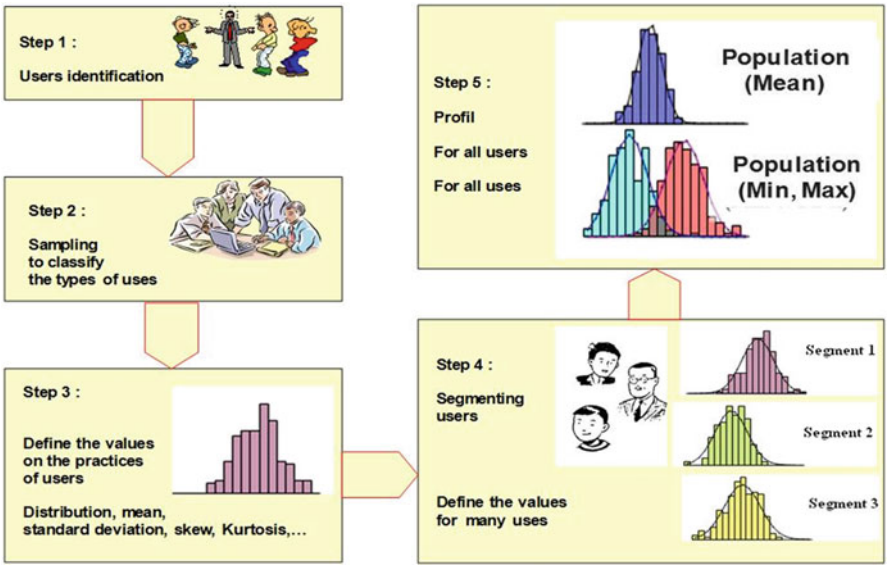

Fig. 1 Taking into account conditions of use

The variety of conditions is the major difficulty encountered in the integration of real condition of use when designing a mechanical component. For example, an equipments model is designed as a response to the needs of a user class (Fig. 1). A user class or class of use (Heuler and Klätschke 2005; Lallet et al. 1995; Leluan 1992a; Ten Have 1989) is often determined based on a profile of life confirmed by a market investigation. Despite the definition of multiple use classes, constructors seek as much as possible on the operating parts of equipments, to make the offer more overall that is to say, to find integrators resemblances between different classes use. The simplest presentation of a class of use or a life profile in the field of transport is by example to determine the number of kilometers traveled by an average user will during a specified period. This number of kilometers is presented as a sum weighted of a set of types of severity often called mission profiles or slices of life (good road, bad road, roundabout, mountain, city, different climatic conditions, etc.). Even if these simplified configurations, predictive calculations of resistance and lifetime require a statement of simplifications and assumptions that lead to the use of safety factors (Clausen et al. 2006) to reduce the risk of defects. Indeed, a class of use (or life profile) is considered by the designer of mechanical components, such as a homogeneous whole. Nevertheless, this homogeneity is accompanied by uncertainties that require consideration in terms of random information. Indeed, it is now proved (Osgood 1982) that a random mechanical stress leads to a lifetime smaller than alternating stress which seems broadly similar.

1.2 Statistical Analysis or Counting Methods of Random Loads

We are interested here in the methods of interpretation of the characteristic parameters of time series (or a discrete graphics representation) to obtain a distribution law of these parameters (Brozzetti and Chabrolin 1986a). From the viewpoint of checking the fatigue of the mechanical components, the extent of variation of the variable load is an essential parameter of the same value as the average stress. Variable loads may come as external actions as internal stresses. In what follows, we shall make no distinction knowing that it is possible to determine the stresses from the variable actions applied to a structure or component, making either quasi-static or dynamic mechanical calculations.

1.2.1 Load Event

The term "load event" (Grubisic 1994) gives rise to a history of stress (also called trajectory). This load event is a load state of service, characteristic of the mechanical system and generating within each component considered, a variation of stimulations.

Examples Included in the transport sector are the following cases:

- Bridge-road: the passage of a vehicle characterized by mass, number of axles, the speed, producing a bias at a particular point of the structure. The passage of the vehicle being a function of several parameters (the surface irregularities of the coating, the transverse position of the vehicle on the item, the weight of the rolling load, speed, etc.).
- Road-chassis: the stresses on the chassis of a vehicle on a road section.
- Marine platform: the action of water depending on the status of storm characterized by the duration, the height, the period, the average direction of waves.

Know the statistical distribution of load events during the intended use of the system or the mechanical component, then leads to the establishment of a statistical distribution law given by the average number of occurrences of each type of event. For a bridge, this distribution is that of the expected traffic; for the chassis of a vehicle, are the driving conditions; and for a marine structure, it will be a weather data on the frequency of storms.

When each load event is characterized by one or more parameters, the long-term distribution is in the form of a histogram, easily representable for one or two parameters (Rabbe et al. 2000a).

In some cases, experience and theoretical modeling used to have this distribution analytically. The histogram obtained is then replaced by a continuous distribution law. The majority of mechanical systems and mechanical components from simple to more complicated are subject to loads distributions often represented by Weibull laws (Chapouille 1980).

For example in the field of land transport, this distribution may relate to severe stresses in a car chassis such as:

$$p\left(C_s > c^*\right) = \exp\left[-\left(\frac{c^*}{c_0}\right)^{\gamma}\right]$$

and

$$p\left(c^* \leq C_s < c^* + dc^*\right) = \frac{\gamma}{c_0}\left(\frac{c^*}{c_0}\right)^{\gamma-1} \exp\left[-\left(\frac{c^*}{c_0}\right)^{\gamma}\right] dc^*$$

$p(C_s > c^*)$ represents the probability of exceeding a threshold c^*; C_s is the random variable representing a severe stress event which can be here a stress due to the passage on a road in poor condition and shown in a significant stress c_0 ; $p(c^* \leq C_s < c^* + dc^*)$ represents the probability of being located around a threshold. It is thus possible to assess the probability that this stress is between c^* and $c^* + dc^*$. For this example, the statistical knowledge of the total number of sections of bad road then used to define a number of instances is to be associated with a given state of stress.

The difficulty of estimating a statistical distribution load event is that any statistical prediction as it relates to natural events (wind, wave, current, etc.) or in-service use of a considered mechanical system or considered mechanical component (traffic on a bridge, resistance of a frame, etc.). This prediction on the probability distribution of load events can be challenged by the emergence of exceptional causes.

Example We may not have anticipated increased traffic on a bridge for special seasonal reasons. Similarly another example, it is always difficult to extrapolate over the long term, the extreme value of a wave height, based on statistical values of wave heights measured in a few months.

1.2.2 Load Spectrum (Grubisic 1994), Histogram

Example Acceleration recorded on the axle as it passes on a test section, the speed of a gust of wind during a given period, etc.

From this trajectory, the problem is to obtain the information necessary to have at a histogram, or a distribution law of stresses that is called the spectrum of loads or stresses (Grubisic 1994), which is in reality only approximate representation of all charges stresses applied. We also note that obtaining load spectrum reduced information, in the sense that you lose the timing of the cycles of load variations. Therefore, the subsequent calculation of the damage (presented in the third part) may not consider any interaction between successive cycles of stress variations due to these loads. It may, however, admit that many events are largely random and it is unrealistic, at the stage of predicting the behavior of mechanical systems and

components claim to have any knowledge of the precise order of appearance, e.g., values of variations ranges of stresses. It thus focuses on the study of the statistical distribution of variations ranges of stresses. And for some applications, the average stress of each cycle is sometimes used. Assume in the following presentation, the overall average stress is zero on the duration of the path.

Statement of Characteristic Data of a Random Loading

Except for some special cases of process (periodic sinusoidal path, stationary narrow band Gaussian process, that is to say with few excitation characteristic frequencies), it is generally difficult to combine with a variations range of stresses of one cycle (Fig. 2). In the case of a very irregular loading path, such as that of Fig. 2, the secondary peaks are problematic. And any a priori definition of how to count variations ranges of stresses may lead to differences in prediction compared to reality, if it is not supported by experimental verification.

The laws of damage based on more or less simple models (Duprat 1997), and the only way to tell if an identification of damaging cycles method is better than another is to correlate the results with those of the studied model of experience where it is possible to achieve (time scale and/or compatible cost, etc.). In fact, the existing methods give results fairly dispersed compared to published (Chang and Hudson 1981) results. For these reasons, the extraction of information from a random stress is to be performed with care. Different types of information to be extracted may occur in the following three forms:

Global analysis: where all the amplitudes of the stress are considered regardless the geometrical shape of the path (amplitude extreme, positive or negative slope, curvature upwards or downwards). This analysis is done using the histogram of the stress or by tracking specific amplitudes in the stress studied.

Local analysis: through the study of extreme values according to the geometrical shape of the path. In this case, the extreme values are separated into four statistical groups: the positive peaks, the trough positive, peaks negative, and trough negative. Amplitudes that do not have a change of direction in the digitized signal are not studied.

Analyses of stress tracts and/or of cycles: When the random stress is considered a constraint, it is useful to think in tract or stress cycle. This definition is consistent with what is done during fatigue tests under sinusoidal stresses that life is measured by the number of cycles. In the case of a sinusoidal stress, a tract concerns only half a cycle. In the case of random stress $S(t)$, defining a cycle is less easy:

- *Definition of a peak and a trough of stress*

  A stress peak S_M (or a trough stress S_m) is defined as the value of a local maximum (or local minimum) of the function $S(t)$. This peak (or the trough) can be positive or negative.

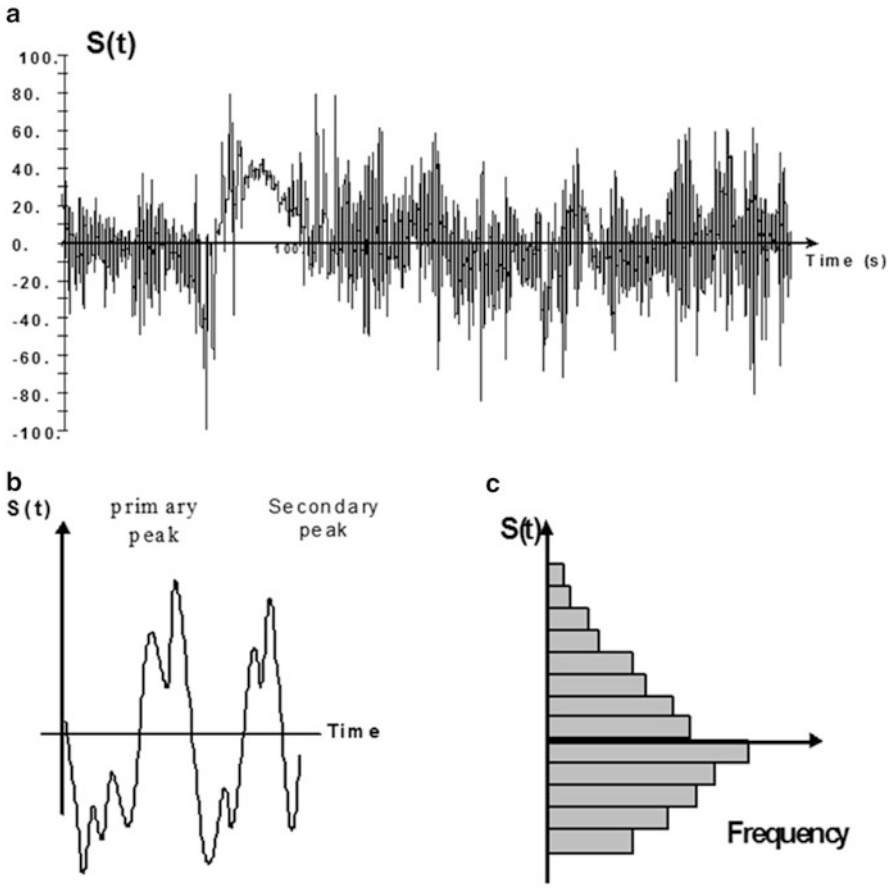

Fig. 2 Viewing a solicitation provided actual use. (**a**) Temporal solicitation, (**b**) detail of signal, (**c**) histogram

- *Definition of a half cycle or one cycle of tract stress variation*

  A tract half-cycle variation of stress is defined by the time between two successive local extreme values of S_M and S_m (the tract of the variation of stress is defined by $S = S_M - S_m$) (Fig. 3a). A tract cycle of stress variation is defined as the time between two successive local maxima whose value is the first S_M and the second is $S_M^{'}$ (Fig. 3a), intermediate local minimum with a value S_m. The extent of variation of stress associated with this cycle is not unique in this case, since it may be taken as

$$S = |S_M - S_m| \quad \text{or} \quad S' = \left|S'_M - S_m\right|.$$

  Another way to define a cycle, and that this is not linked to the counting of the peaks and troughs of a path, is related to the time interval between two zero crossings and by increasing value (or decreasing values) of the path (Fig. 3b).

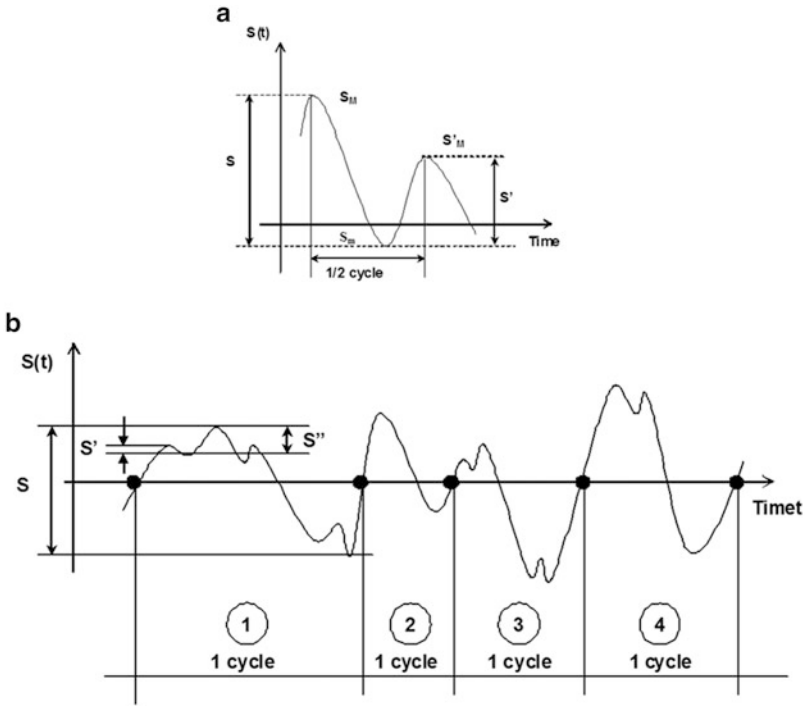

Fig. 3 Definition of characteristics of stress. (**a**) Half cycle definition, (**b**) series of cycles

The example of Fig. 3b with local peaks and local troughs shows the difficulty in defining one cycle and the tract of variation of stress associated with this cycle. Only the cycle no. 2 in the figure is used to define a single tract of variation of stress associated with this cycle.

In summary, three pieces of information must be seen from a random loading: the amplitudes that have imposed load considered (overall analysis), specific amplitudes observed by zooming effect and that reflect the severity of loading (local analysis), and finally tract or extracts cycles of loads studied. And counting methods (Lalanne 1999a) can be divided into three groups: global methods, local methods, and the methods of counting matrix.

Counting Global Methods

The main global counting methods (Lalanne 1999a) are: counting by class and method count overruns levels. For each counting method, an application will be presented around the stress shown in Fig. 4a.

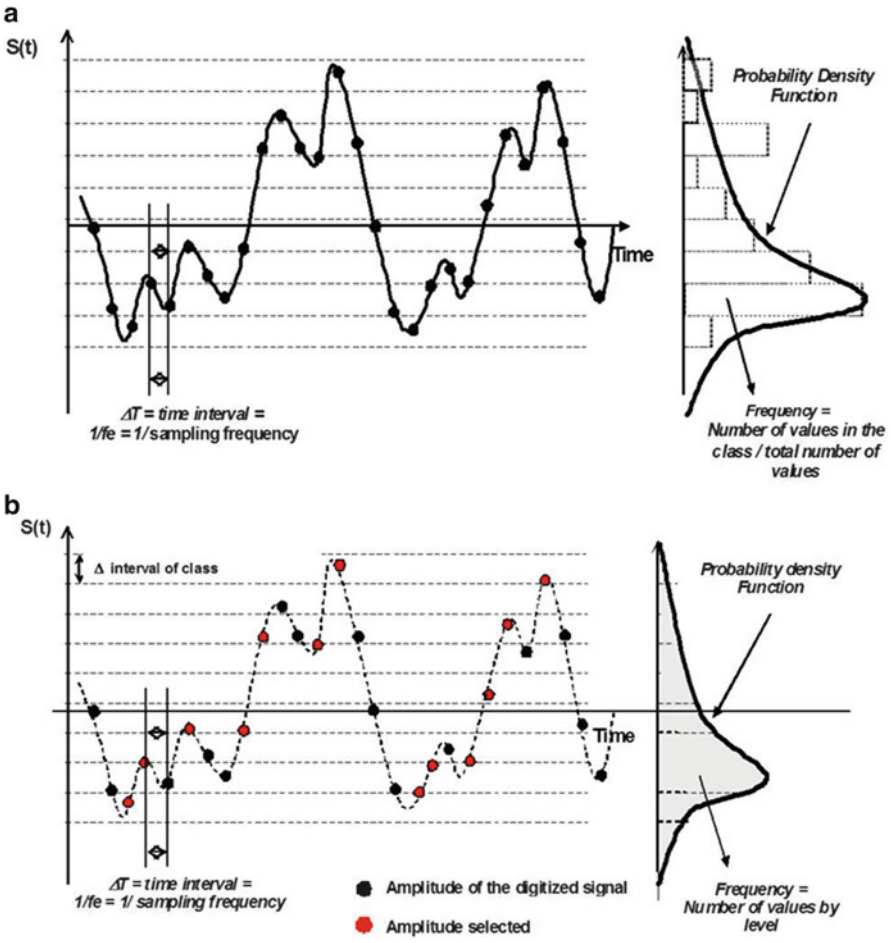

Fig. 4 Descriptive statistics of stress. (**a**) Realization of histogram, (**b**) definition of probability density function

Histogram or Holding Time in a Class of Amplitudes

This method considers the digital signal recorded as a statistical sample not knowing the temporal aspect. The sample is grouped into classes of amplitudes (Fig. 4a, dashed horizontal lines). In this case, no distinction is made between the extreme values and others. The advantages of this method reside in the immediate possibility of statistical modeling and propose a model of probability density (right side of Fig. 4a). Since between two successive points, there is a not predefined time by the method of measurement, the number of points recorded in a class when multiplied by the time step gives the total holding time of the stress studied in this class of amplitudes. This counting method should be reserved only for homogeneous stress

(or whose source is considered homogeneous) that is to say, if no significant change in the nature of loading. Indeed, this method is very dependent on the speed (first derivative of the curve considered on a path with a specific dynamic signature) and the acceleration (second derivative) of the stress studied. In the case where the stress has several types of information (related to the braking, cornering, various loads, etc.), the signal loses its homogeneity and the counting class will be altered by these class different uses which dynamic signature is not the same. Figure 4a shows a digitized stress where 28 points and 9 classes of amplitudes are defined. The counting class (from the class below) leads successively to 2, 7, 3, 5, 1, 2, 5, 1, and 2 amplitudes per class.

Counting the Number of Level Crossing

This method, like the previous one, calls for predefined amplitude classes (Fig. 4b). Counting, for a given level, is triggered when the signal exceeds a level with a positive slope (hence the name level crossing). A count of the number of given level crossing is only relevant if an attitude selection of small oscillations is defined. These small oscillations can provide loads staffing (number) without interest from the point of view of calculating the damage and calculating life. And for counting the number of level crossing increment signal noted Δ is defined. It is often in the case of a mechanical component, interval stress below a fatigue limit set to a Wöhler curve (Leybold and Neumann 1963). This increment is considered Δ a threshold reset in the counting process. Historically, several counting methods have been proposed. The most interesting method has only one level if the stress has already gone through at least once this threshold Δ, irrespective of nature of slope. It should also be remembered that the counting is done with a digitized signal, and a proximity rule should be implemented to count very close to the levels determined amplitude. This counting method allows—as the previous one—to build a model of probability density. The application of this method focuses on the levels defined by the class boundaries. Count per level (with the solicitation of Fig. 4b, from low level) leads successively to 0, 0, 2, 1, 0, 1, 1, and 2 level overruns.

Counting Local Methods (Local Events)

Extreme values (peaks and troughs) of a random stress occur from four different families by:

- Positive maximum values preceded by a positive slope (peak > 0)
- Negative minimum values preceded by a negative slope (trough < 0)
- Negative maximum values preceded by a positive slope (peak < 0)
- Positive minimum values preceded by a negative slope (trough > 0)

Figure 5 illustrates these four families of amplitudes. As for the global analysis, grouping into classes for each family gives the possibility to build a model of probability density by type of extreme values. The result of this counting method around the stress shown in Fig. 5 leads, starting from the low class of the nine amplitude classes, to the results in Table 1.

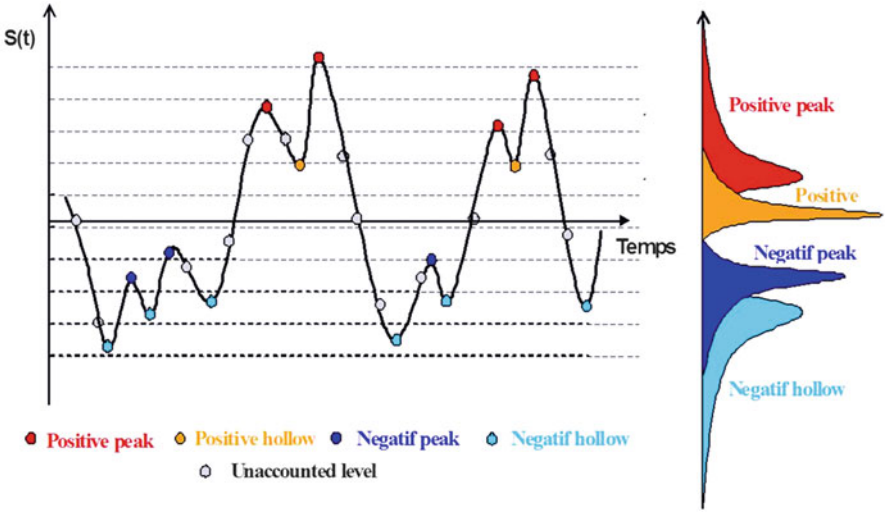

Fig. 5 Descriptive statistics with local events

Table 1 Local counting method

Classes	Trough < 0	Peak < 0	Trough > 0	Peak > 0
1[a]	1	0	0	0
2	4	0	0	0
3	2	2	0	0
4	0	1	0	0
5	0	0	0	0
6	0	0	0	0
7	0	0	2	1
8	0	0	0	1
9	0	0	0	1

[a]The lowest class

Counting Matrix Methods

Matrix counting methods take into account the evolution of the mean stress and/or involve the concept of stress cycle.

Counting Tract Between Peaks and Troughs

A tract (Fig. 6a) is defined as the difference between the given maximum and minimum (negative range), or between a given minimum and maximum (positive range). This method has half cycles. A variant of this method consists in associating with each cycle, the average of the positive and negative tract (to create tract average

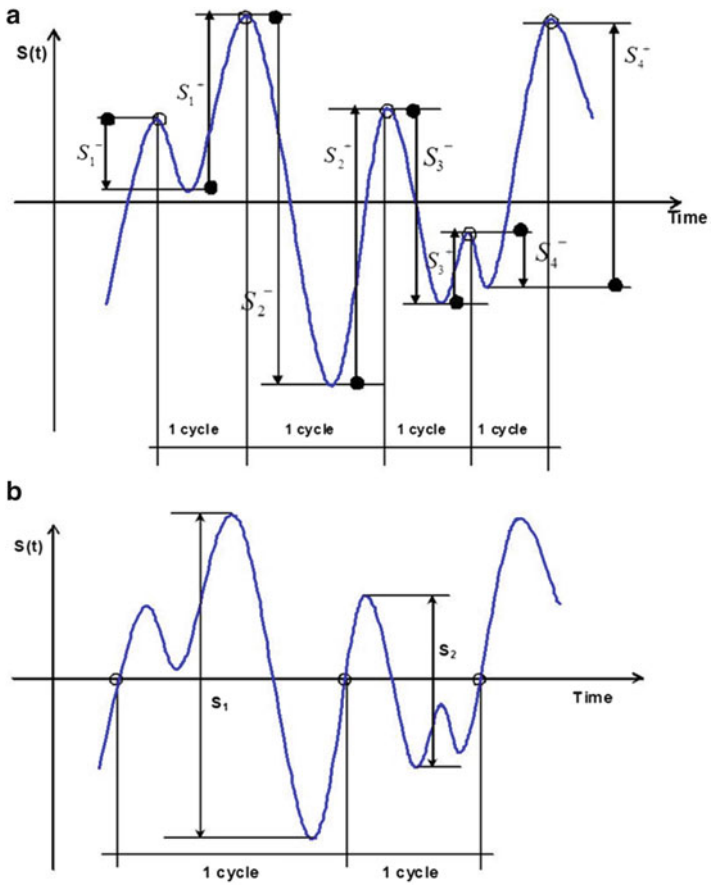

Fig. 6 Counting tracts of stress. (**a**) Counting between peaks and troughs, (**b**) counting means cycles

counts). The results of this counting method for the solicitation studied in this paragraph are shown in Fig. 6a. Indeed, the values S_1^-, S_1^+, S_2^-, S_2^+, S_3^- , S_3^+, S_4^-, et S_4^+ are the only tracts identified in this solicitation.

Counting Means Cycles

A cycle is defined by means the time between two zero crossings by increasing value (positive derivative). The tract of variation of stress S for this mean cycle is defined by the maximum of the local maxima and minimum of local minima inside this mean cycle (Fig. 6b). Just as the previous method, the counting results of this method are shown in Fig. 6b. Indeed, this counting method locates two identified cycles by S_1 and S_2 tracts, respectively, corresponding to the values S_2^- and S_3^- of the previous method.

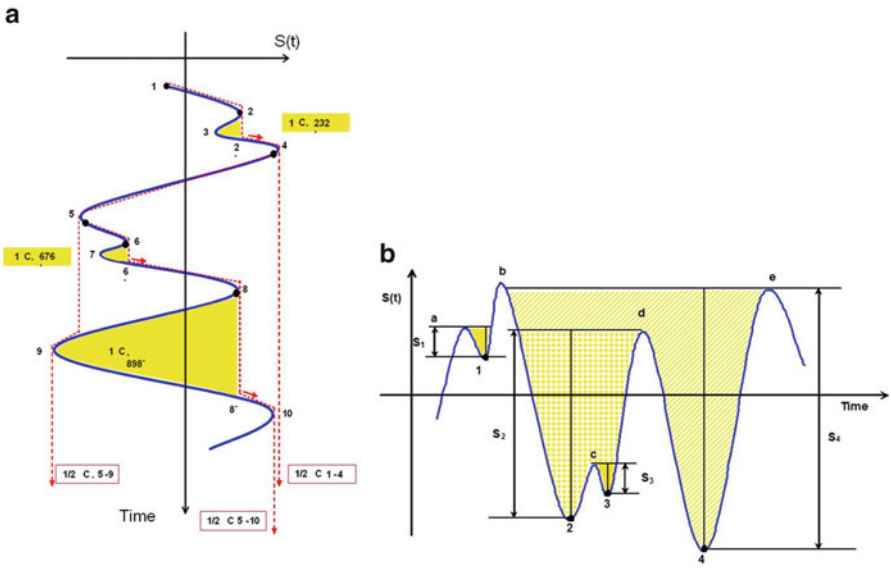

Fig. 7 Global cycle count of stress. (**a**) Rainflow method, (**b**) tanks method

"Rainflow" Method

This method takes into account all sequences of stress and in particular, it has all the secondary stress variations of the trajectory. It takes into account the half cycles and cycles by different, from that which was described in Sect. 2.3.3.1, way. Its name comes from how to identify cycles by the flow of a drop of water that slides along the path from top to bottom (Fig. 7a, vertical time axis to image representation). Whenever a drop of water leaves the path, a new cycle is initiated from the next summit. Counting cycle stops when the drop is blocked (the drop of water cannot follow the same path a path previously followed by another drop). If the end of the path is reached without blocking, there is only one half cycle. This method is cumbersome to implement and it does not lend itself easily to statistical mathematical modeling and the use of statistical properties of the trajectories of a random process. In the case of Fig. 7a, three cycles are observed (232′, 676′, and 898′) and three half-rings (1–4, 5–10, 4–9).

Tank Method

This counting method is similar to the previous one. It also has the advantage of taking into account all sequences tracts of stress variation. This method takes its name from the hydraulic analogy it presents with emptying a tank. One can imagine that all the pockets the water path is filled (Fig. 7b, now the time axis is shown horizontally). Was identified by decreasing values all troughs and imagine that each of these troughs has a drain valve. The tap of the lowest trough l is open, the tank

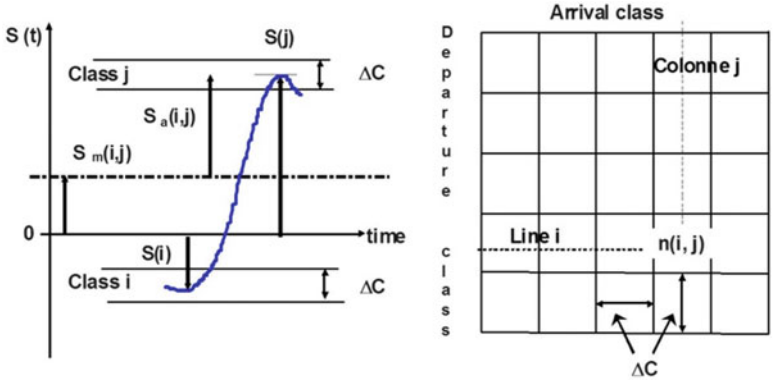

Fig. 8 Construction of MARKOV matrix

empties, leaving the other pockets filled with water. It does so by opening the valve of the next lowest trough and so on until you have emptied every pocket. You identify for each difference in height of water, a tract of variation of stress. A tract of variation of stress is cycle. For example, four reservoirs are detected on the stress of Fig. 7b. Each tank defines a stress cycle. The detected tanks are:

- The tank defined by the level (a) and the trough (1)
- The tank defined by the level (d) and the trough (2)
- The tank defined by the level (c) and the trough (3)
- The tank defined by the level (e) and the trough (4)

This method gives results similar to those obtained with the previous method. From the point of view of its mathematical formulation, it is easier to implement, but it nevertheless has the same disadvantages as the previous one.

Method of Transition Matrix or MARKOV Matrix

This method facilitates the counting of half cycles of stress. It is easier to automate. It leads to the construction of a transition matrix called MARKOV matrix (Lieurade 1980a; Kouta and Play 2006). The latter is obtained by the following steps (Fig. 8):

1. Temporal stress studied is divided into classes of amplitudes width ΔC. This width is considered as a threshold for filtering because all fluctuations within a class of amplitudes are ignored. The class width is often, in the case of a mechanical component, in a range below a stress fatigue limit set to a Wöhler curve (Leybold and Neumann 1963) (similar to the threshold Δ defined in Sect. 2.3.1.2).
2. Pour démarrer le comptage, la classe d'appartenance de la première amplitude observée, est détectée. Cette classe est considérée comme une classe de départ. La classe d'arrivée est déterminée quand le signal atteint un extremum.

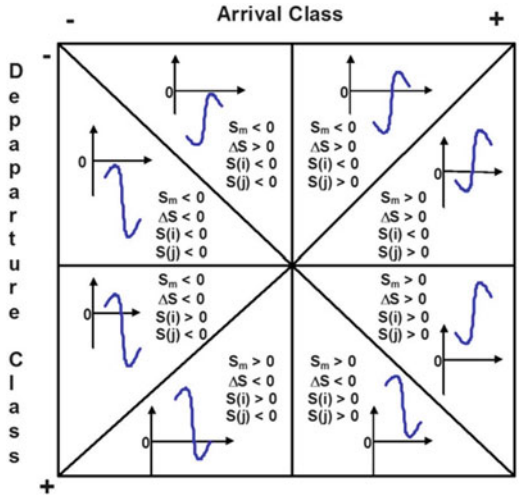

Fig. 9 Subdivision of MARKOV matrix

3. Thus, the horizontal dimension (row i) of the transition matrix (right part of Fig. 8) shows the starting classes and the vertical dimension has the arrival classes (column j). Box crossing the line i and column j is used to indicate the number $n(i, j)$ times the transition stress was observed.
4. The MARKOV matrix is thus transitions to an extremum of another ($S(i) \rightarrow S(j)$). The alternating amplitude $S_a(i, j)$, the average amplitude $S_m(i, j)$ of the transition, and tract $\Delta S(i, j) = S(j) - S(i)$ can be calculated.

$$S_a = \frac{S(j) - |S(i)|}{2} - S_m\,(ij)$$

$$S_m\,(i, j) = \frac{S(j) + |S(i)|}{2}$$

Figure 9 explains the transitions detected in the various subparts of a Markov matrix. This particular figure shows that most of the severity of a stress (with nonzero average value) is located in the top-left quadrant and the lower right quarter. Figure 10 shows a MARKOV matrix obtained for the deflection of a right front axle of the industrial vehicle. This stress is observed upon passage of the vehicle on a specific test section with five concrete bumps.

Conclusion on the Counting Methods

The different counting methods give different results, by the type of path considered. The method of counting of cycles means produces the same results for the three cases of Fig. 11a. The method of counting the peaks gives the same results for the

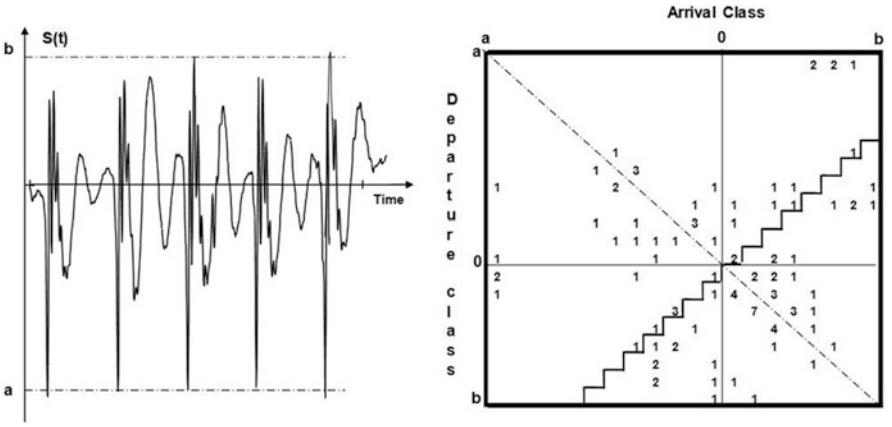

Fig. 10 MARKOV matrix for the deflection of the front right axle of a motor vehicle (Measured on a section consists of five bumps in concrete)

case (2) and (3) of Fig. 11a. Drop of water counting method or tank counting method and tracts between peaks and troughs give very different results for the two paths in Fig. 11b.

Currently, we do not have a number of published experimental tests enough on material fatigue under random stresses actual reasonably to conclude on the choice of method. However, some laboratory studies (Société française de métallurgie (Commission fatigue) 1981; Gregoire 1981; Olagnon 1994) show that in specific cases the method of counting the peaks and the counting method of the drop of water (counting method similar to the tank) give satisfactory results. So many regulations on fatigue verification of structures, systems, and mechanical components currently recommend, take the method of counting the drop of water. But it should take precautions to extrapolation of complex industrial cases. Remember that it is not enough to properly count the events, but it is also essential to develop approaches to mathematical modeling, probability, and statistics. These models offer several opportunities for engineers, for example:

- Objective classification of different types of stresses
- Possibility (after classification) build rules correlations between sources of stresses
- Production significant bench tests and numerical calculations of fatigue representative from actual conditions of use

Similarly, these models will be needed to establish predictive methods of calculating lifetime or to perform reliability analyses.

The difficulties in this type of modeling with some counting methods (counting of the drop of water or tanks, for example) lead to consideration of other methods such as the level crossing or the matrix MARKOV (Klemenc and Fajdiga 2000; Rychlik 1996; Doob 1953). When comparing different methods for counting a given

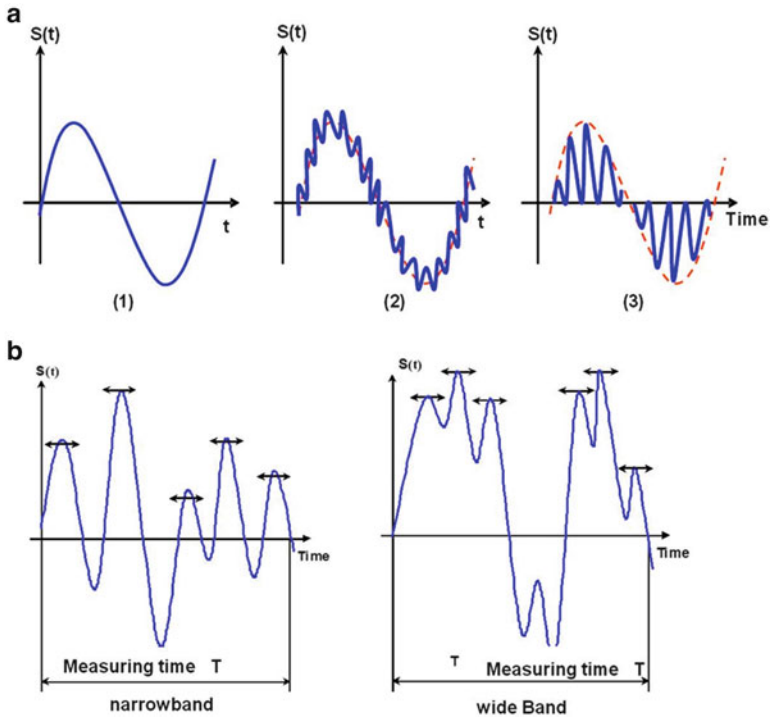

Fig. 11 Different scenarios of stress. (**a**) Comparison of counting methods, (**b**) solicitations with narrow or wide band

historical of use, it must examine the sensitivity of the methods taking into account the following parameters:

- Number of cycles detected.
- Detection of major cycles.
- Consideration of small tract of stress variation.
- Taking into account the average values of each cycle.

Finally, in the context of a particular business, you must choose a representative method load considered and that is consistent with the results of the experiment. But also the choice of the method will be conditioned by the calculation methods implemented in the future to perform the calculations lifetime. Representative path stress event is similar to a random process which is not known a priori, the form that its realization. The mathematical tools needed to solve these problems relate to the theory of probability and statistical properties related to the trajectories of random processes (Parzen 1962; Preumont 1990).

1.3 Frequency Analysis

The frequency analysis (Arquès et al. 2000) provides the notion of Power Spectral Density (PSD). Before developing the concept of PSD, some precautions are necessary for the representation of developments. These precautions are about of nature of stress to study. It is assumed that the path on the stress process $X(t)$ satisfies the following assumptions:

- The process $X(t)$ is continuous over the observation time chosen equal to a time unit that is referred to as the reference period.
- First $\dot{X}(t)$ and second derivatives $\ddot{X}(t)$ of the path $X(t)$ are continuous processes on the observation time.
- The process $X(t)$ is centered, that is to say the average $M(X(t))$ is zero. If $X(t)$ is not centered, the transformation is performed: $X(t) \rightarrow (X(t) - M(X(t)))$.
- The process $X(t)$ has independent statistical properties of time. The process is stationary. Statistical properties by means of spectral moments (defined later in the text) of $(X(t))$ of order 0, 2, and 4.
- The process $X(t)$ is Gaussian, that is to say that the random variable $(X(t_1)$ and $X(t_2), X(t_3), \ldots, X(t_n))$ on $t_1, t_2, t_3, \ldots, t_n$ follows a Gaussian distribution law.
- The statistical characteristics of the random variable at a time are the same as those of the time stress.

1.3.1 Power Spectral Density

PSD is determined according to the frequencies that appear in the stress, following a well-known process (Fig. 12a) (Plusquellec 1991; Borello 2006). This gives a power spectrum. In addition, the quadratic mean of the amplitudes (or variance) is defined. The latter is often called the intensity of the stress or RMS (Root Mean Square). The determination of the PSD is considered material if it is known that stress for a component at a given observation point is caused not only by external forces but also by the interaction effects of the component studied with the different elements system to which it belongs. For example, Fig. 12b (Buxbaum and Svenson 1973) shows the PSD of a record on a mechanical system in automotive signal. Two characteristic frequencies of the frame and of the suspension are identified.

The determination of the power spectrum of a random stress observed in the actual conditions of use of a mechanical component provides two types of information:

- Distinction between the different sources of stress measured.
- Contribution of each frequency to the intensity of the stress, defined rms.

According to WIENER–KHINTCHINE (Max 1989), PSD of a stationary process, as noted, is defined as the frequency distribution of the average energy of a process $X(t)$ where t represents time. $\varnothing_{xx}(\Omega)$ is connected to its autocorrelation function $R_{xx}(\tau)$.

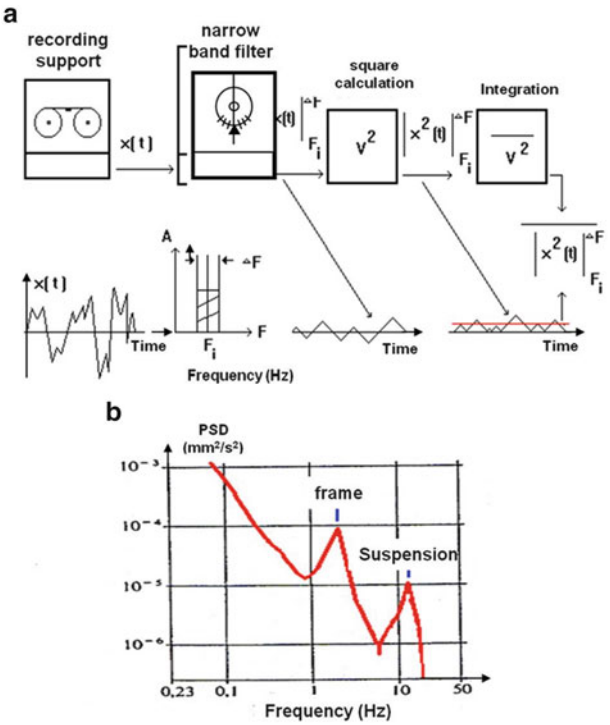

Fig. 12 Obtaining the Power Spectral Density (PSD). (**a**) Numerical procedures, (**b**) PSD example (Max 1989)

For a stationary process, we have:

$$R_{xx}(\tau) = \int_{0}^{+\infty} x(t) \times x(t-\tau)\ dt \tag{1}$$

Thus,

$$\varnothing_{xx}(\Omega) = \frac{1}{2\pi} \int_{-\infty}^{+\infty} R_{xx}(\tau)\, .e^{-j\,\Omega\tau}\ d\tau \tag{2}$$

and

$$R_{xx}(\tau) = \int_{-\infty}^{+\infty} \varnothing_{xx}(\Omega)\, .e^{j\,\Omega\tau}\ d\Omega \tag{3}$$

So for the same process, but with a zero mean, the expression of the variance (or the RMS in this case) is obtained by imposing $\tau = \mathrm{o}$ in the following relationship:

$$R_{xx}(o) = \int_{-\infty}^{+\infty} \varnothing_{xx}(\Omega)\ d\Omega = \sigma_X^2 = E\left[X^2(t)\right] = \mathrm{RMS} = m_0 \tag{4}$$

This last result is appointed first spectral moment. Two other spectral moments are defined by

$$m_2 = -\ddot{R}(0) \quad \text{and} \quad m_4 = R^{(4)}(0)$$

$R^{(4)}$ is the fourth derivative.

In the case of the process discussed here, m_0, m_2, and m_4 are, respectively, the same as the variance of the stress, of its first derivative and its second derivative as follows:

$$m_0 = V\left(X(t)\right), \quad m_2 = V\left(\dot{X}(t)\right) \quad \text{and} \quad m_4 = V\left(\ddot{X}(t)\right)$$

In practice, the PSD is written as follows:

$$\varnothing_{xx}(\Omega) = \lim_{T \to \infty} \frac{1}{2\pi T} \left[\left| \int_{-T/2}^{T/2} X(t).\mathrm{e}^{-j\Omega t}\ dt \right|^2 \right] \tag{5}$$

This relationship provides an interesting interpretation especially in the case of a single measurement. In practice, the signal strength (stress) is determined by bands of frequencies (the most selective possible). This intensity is represented by the area bounded by the time signal curve for each frequency. In general, this is characterized by intensity variations of the curvature of the signal-time trajectory. Figure 12a diagrammatically shows the determination of the PSD. In this case for a real signal, the autocorrelation function is real and even, it is the same to the PSD $\varnothing_{xx}(\Omega)$. Relations Eqs. (2) and (3) can be written:

$$\varnothing_{xx}(\Omega) = \frac{1}{\pi} \int_0^{\infty} R_{xx}(\tau) \cos(\Omega\tau)\ d\tau$$

$$R_{xx}(\tau) = 2 \int_0^{\infty} \varnothing_{xx}(\Omega) \cos(\Omega\tau)\ d\Omega \tag{6}$$

Figure 13a (Rice et al. 1964) shows various forms of random stress and their associated PSD. The stress 1 is almost sinusoidal and the PSD is centered around

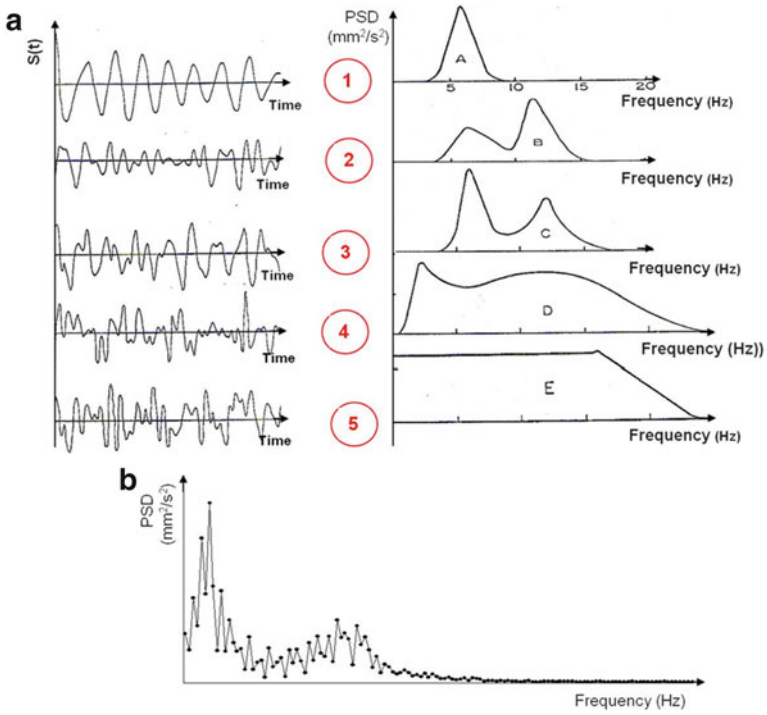

Fig. 13 Example of PSD. (**a**) Different kinds of stresses, (**b**) PSD for stress of Fig. 10

of the main frequency, it is a very uniform stress. The two well-identified peaks of DSPs of stress 2 and 3 are well explained by the presence of two frequencies that appear on the requests presented. The highest amplitudes of DSPs 2 and 3 indicate that these two frequencies are not the same energy signature for each stress. For four and five solicitations, all observed frequencies have almost the same importance. The stress 4 shows a frequency that differs from the other in the low frequency range. The stress 5 has a practically constant energy level whatever the frequency and this frequency range on a wide. And PSDs provide information on the statistical nature of the studied stresses and are indispensable when it comes to a classification of different mission profiles or classes of use of a component or a mechanical system. Its importance is even greater than it is thanks to PSDs that testing laboratories to reproduce test benches solicitations recorded in real conditions of use (Tustin 2001).

Figure 13b shows the PSD on the measurement of a movement, shown in Fig. 10. We see that this is a scenario loading close enough stress 4 shown in Fig. 13a. Indeed, despite the presence of a significant noise energy level, there is a frequency that is distinct from the other and has a high energy level. Physically, this is explained by the five shocks obtained when the vehicle passes over bumps of concrete.

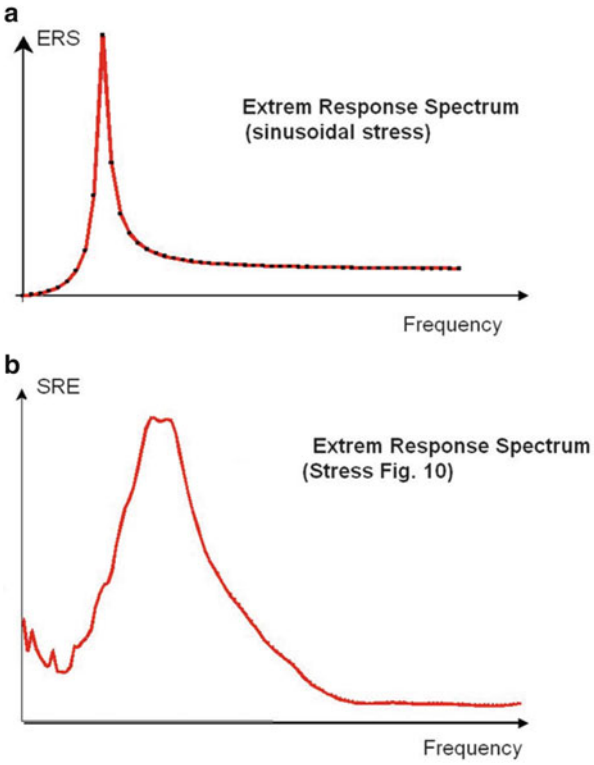

Fig. 14 Example of extrem response spectrum (ERS) (**a** sinusoidal stress, **b** stress Fig. 10)

1.3.2 Extrem Response Spectrum

Extrem response (ER) (Lalanne 1999b) is characterized by the quantity

$$\mathrm{ER} = \left(2.\pi.f_p\right)^2.Z_\mathrm{m}$$

Z_m is the maximum response once met, the probabilistic sense, during the duration of the random excitation. The Extrem Response Spectrum (ERS) is the graph of changes in ER based on the natural frequency of the system with one degree of freedom f_p, for a given damping factor ξ. The extreme response is representative of the largest stress S_m suffered by the component assuming $S_\mathrm{m} = K.Z_\mathrm{m}$ ($K =$ spring constant).

Figure 14a shows spectrum of the extrem response for a sinusoidal stress and Fig. 14b shows the stress of the ERS shown in Fig. 10.

Obtaining spectrum extreme response requires the definition of the statistical distribution of extreme values of the stress studied. This is the subject of a paragraph of Part 2. The process of obtaining the ERS and applications are subject to Annex C of Part 2.

1.4 Conclusion

Statistical analysis is mainly represented by the counting methods. Frequency analysis is mainly determined by consideration of the PSD and extreme spectral response. The combination of the two analyzes can be considered a stress studied as a random process. Indeed, the uptake of random stress a random path will allow providing probabilistic modeling of a number of methods of numeric counts. These probabilistic models can also include elements of the frequency analysis and in particular PSD of the stress studied.

2 Random Loadings Modeling

The ultimate goal of these three parts is to develop essential methods and essential tools to predicting the lifetime of mechanical components. In the first part, statistical analysis and frequency analysis allowed to have a representation of the stresses applied to a system or a mechanical component. This will allow the second part to move from these representations for models with as ulterior objective to calculate the lifetime. Two types of models will be discussed in this article. The first is based on statistical and probabilistic approaches. The second incorporates an interaction between statistical analysis and frequency analysis.

2.1 Probabilistic Modeling of the Histogram of a Random Stress

The transition from the statistical analysis to a random stress probabilistic modeling with mathematical analysis is always tricky. Indeed, the purpose of modeling random loads is to determine a theoretical probability of occurrence of events, from the observation of a series of values $(x_i)_N$ of a random variable (X). If descriptive statistics seeks to pass judgment on the random variable with respect to preselected values, mathematical statistics seeks to make judgments about the probability of different values. The histogram (Fig. 15a) becomes a "density estimator" and accumulations diagram (Fig. 15b) is "probability estimator" (distribution function). Whichever method of synthesizing a random stress, the information collected can be probabilistic modeling (Saporta 1990). In the remainder of this section, the modeling of the conventional histogram is presented. This can also apply to all methods of unidimensional digital counting. Two-dimensional models are not discussed in this article. Thus for stress studied, the probability of overrun for any level is obtained. Similarly, after modeling the probability density $f_X(x)$ and distribution function $F_X(x)$, all the basic statistical techniques may be applied (including laws minimum and maximum).

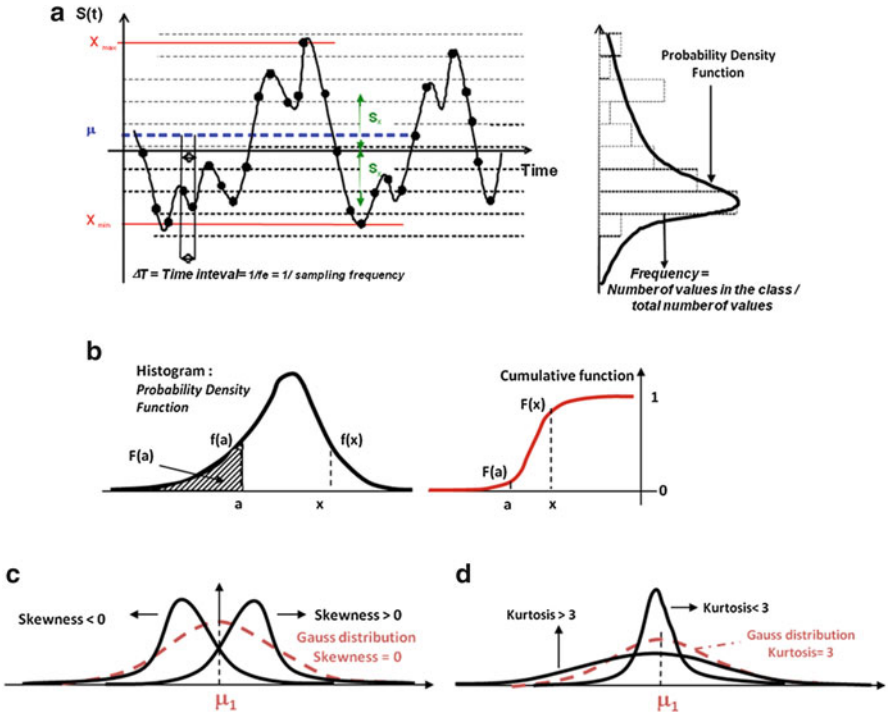

Fig. 15 Introducing the stress reference. (**a**) Example of stress, (**b**) definitions, (**c**) skewness, (**d**) kurtosis

$$\text{Probability}\quad (X < x) = F_X(x) = \int_{-\infty}^{x} f_X(u)\,du \quad \text{with} \quad \int_{-\infty}^{+\infty} f_x(x)\,dx = 1 \qquad (7)$$

In practice, the distribution of X is continuous, the density $f_X(x)$ is obtained from the observed series $X_1, \ldots, x_N$. Call f_N the function that maps x real, the number $f_N(x)(=f_i)$ equal to the height of the rectangle which is relative to the class containing x (Fig. 15a). The purpose of modeling is to say that for all x, the two values $f_N(x)$ and $f_X(X)$ are "close." Some fit tests are used with wariness in the interpretation of a statistical test (χ^2, Kolmogorov tests (Fauchon J Probabilités et statistiques INSA-Lyon)). Given the variety of histograms encountered during the processing of random stress, two modeling approaches can be taken: modeling on the model of *K*. Pearson (Guldberg 1920; Kendall and Stuart 1969) or modeling on the model of Gram-Charlier and Edgeworth (Edgeworth 1916; Charlier 1914). The data to start for these two approaches are shape indicators of stress studied. These indicators are the minimum, maximum, average, standard deviation, asymmetry, and kurtosis stress studied (Fig. 15c, d).

2.1.1 Shape Indicators of a Random Loading

Figure 15a shows schematically a random stress. $x_{\min}$ and $x_{\max}$ are, respectively, the minimum and maximum values recorded:

$$x_i = x(t_i),$$

The amplitude x_i is measured time t_i knowing that:

$$t_{i+1} = t_i + \Delta t = t_i + \frac{1}{f_e}$$

With Δt time step; $f_e = \frac{1}{\Delta t}$ sampling frequency.

All of these values are the stress studied. The considered average is the arithmetic average:

$$\overline{x} = \mu_1 = \frac{1}{n}\sum_{i=1}^{n} x_i \tag{8}$$

It is the center of gravity of digitized values. The considered standard deviation is the mean of squared difference:

$$s_x = \sqrt{\mu_2} = \sqrt{\frac{1}{n}\sum_{i=1}^{n}(x_i - \overline{x})^2} \tag{9}$$

This is a calculation of the inertia of the stress dispersion studied about the central tendency or its center of gravity. The asymmetry and kurtosis are defined with respect to the law of Gauss.

The asymmetry factor for the law of Gauss is zero; the kurtosis factor is equal to 3. Figure 15c shows a Gaussian distribution and the consequences of a nonzero asymmetry. If the statistical distribution of random stress does not follow a Gaussian distribution, the asymmetry factor indicates the spreading in the right or left of the mean of the distribution.

The kurtosis factor indicates the crushing of the distribution or concentration around a given amplitude (Fig. 15d). Table 2 presents the expressions of asymmetry and kurtosis (Johnson and Kotz 1969).

Centered moment of order r: μ_r, is obtained differently if the evaluation is done from a random stress or a probability distribution. Table 3 presents the two methods of calculation.

In the case of a random stress, a new form factor is defined and is called irregularity factor I. This factor is the ratio of the number of zero crossings N_0 of the focus signal and the number of contained extrema N_e in the studied stress.

Table 2 Expression of asymmetry (skewness) and kurtosis

Parameter	Skewness	Kurtosis
English literature	$\beta_1 = \mu_3^2 \Big/ \mu_2^3$	$\beta_2 = \mu_4 \Big/ \mu_2^2$
French literature	$G_1 = \dfrac{\mu_3}{\mu_2^{3/2}} = \text{signe}\,(\mu_3)\,(\beta_1)^{1/2}$	$G_2 = \beta_2 - 3$

Table 3 Calculation of central moment of order r

Parameter	From a random stress	From a probability distribution $f_x(x)$
Central moment of order r (μ_r)	$\mu_r = \frac{1}{N}\sum_1^N (x_i - \overline{x})^r$	$\mu_r = \int (x - E(X))^r f_x(x)\, dx$[a]

[a] $E(X) = \int x f_x(x)\, dx$ represents the expectation of the random variable X (or average x). Note that these integrations are performed on the domain of definition of x

$$I = \frac{N_0}{N_e} \quad I \text{ is between 0 and 1}$$

More I nears 1, the more regular of the stress is important. Thus, almost each extremum is always followed by a zero crossing (Fig. 16a). In this situation, the measure in question is described as "stress narrowband." When I nears 0, the regularity of the stress becomes lower. Thus, between two zero crossings level, the signal goes through many extrema on the same sign (Fig. 16b). In this situation, the measure in question is described as "stress broadband." The irregularity factor gives an important indication of the temporal evolution of stress, what other form factors completely unaware. In Appendix 4, factors of irregularity are defined. They will have a liaison role between statistical modeling and frequency analysis of a random stress.

2.1.2 Pearson Approach for Obtaining the Probability Density

In the study of shapes distributions frequently observed, normal or Gaussian distribution occupies the place of "generator" function. Pearson (Kendall and Stuart 1969; Johnson and Kotz 1969) proposes a differential equation which includes in its solutions a set of curves of probability density.

$$\frac{1}{f_X(x)} \frac{df_X(x)}{dx} = \frac{x + a_0}{b_0 + b_1 x + b_2 x^2} \tag{10}$$

With $f_x(x)$ probability density function of (denoted as p.d.f), a_0, b_0, b_1, and b_2 are parameters to be estimated and are dependent indicators shape of stress studied (mean, standard deviation, asymmetry, and kurtosis).

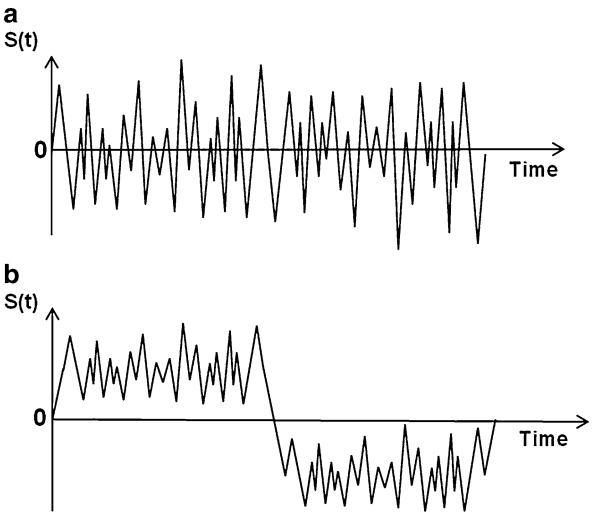

Fig. 16 Characterization stresses depending on the irregularity factor *I*. (**a**) Stress with an irregularity factor $I \cong 1$, (**b**) stress with an irregularity factor $I \cong 0$

Different values of these give a series of "types" of solution (Jeffreys 1961) that generate a set of distribution curves. Several solutions of Eq. (10) correspond to conventional distribution curves with particular values of β_1 and β_2. Other solutions take into account family values β_1 and β_2.

2.1.3 Introduction of the Pearson System Solutions

If a random variable X has an average m_X and a standard deviation s_X, $Y = (X - m_X)/s_X$ is centered reduced random variable associated with X. The average of Y is zero; the standard deviation of Y is 1.

For a random variable centered reduced, the Pearson system leads to seven types of theoretical solutions. These solutions are defined in terms of asymmetry and of kurtosis.

Figure 17 shows the chart of system solutions Pearson. The lines D1 and D4 give the limits of the solutions obtained. Each limited area between two lines corresponds to a probability density model. The lines D2, D3, D5, and D6 correspond to particular probability laws. For $\beta_1 = 0$ and $\beta_2 = 3$, we find the Gaussian (or normal distribution). The solutions obtained on straight D2, D3, D5, D6, or a particular point N are cases very difficult to obtain figures in reality. Indeed, it is almost impossible to find numerical values of β_1 and β_2 which are exactly the equations straight. For this reason and in practice, the solutions of the Pearson system can be reduced to three characteristics solutions: Beta1 law, Beta2 law, and Gamma distribution.

The Beta1 law in the area between the straight lines D1 and D2. The Beta2 law in the area between the lines D3 and D4. The Gamma distribution in the intermediate zone between areas treated with Beta1 and Beta2 laws.

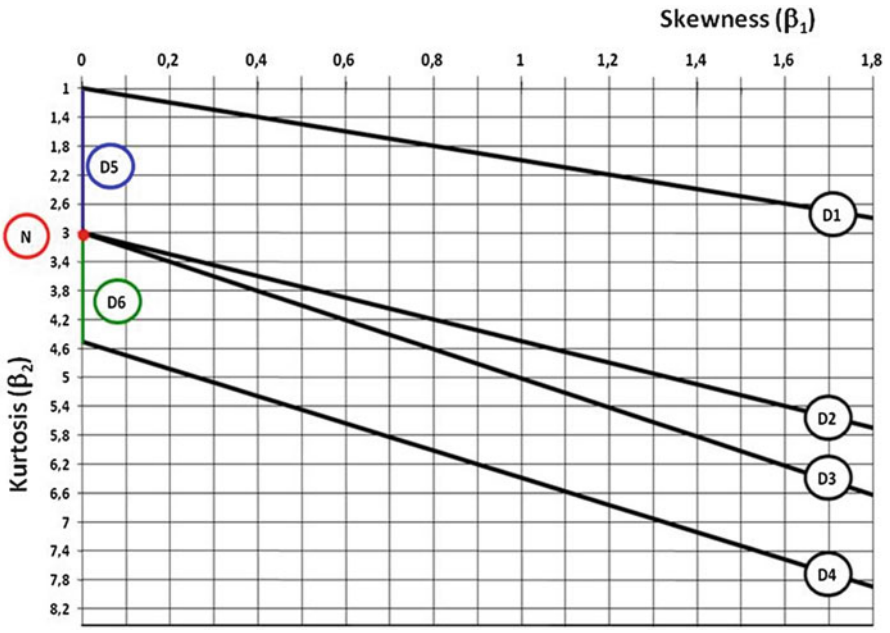

Fig. 17 PEARSON abacus

Appendix 1 presents main solutions of the Pearson system and the laws of probability alternatives that are easier to handle and which estimate their parameters is easier.

Synthesis and Conclusion of the Pearson System

The Pearson system has the advantage of specifying that a random stress can be modeled by three laws presented earlier. In the case where several random stresses from the same environment use must be considered, it is easier to have to provide a single model probability density. Thus, other modeling means are developed with a representation of the distribution curves by the series expansion technique. Gram-Charlier and Edgeworth (Kendall and Stuart 1969; Johnson and Kotz 1969) have developed an expansion method which allows to obtain functions of arbitrary distributions based on the technique of the series expansion, around a continue and known distribution called generator function. The expansion of the normal distribution using a series expansion of Taylor series category.

2.1.4 Gram-Charlier–Edgeworth Approach for Obtaining the Probability Density

Recall that if $f(x)$ is a probability density function, a series function (Eq. (11)) defines a probability density if it justifies the two necessary conditions:

$$g(x) \geq 0.0 \quad \text{and} \quad \int_{-\infty}^{+\infty} g(x)\, dx = 1.$$

In this case, $g(x)$ has some pluralitings $k_1, k_2, \ldots$ (Kendall and Stuart 1969):

$$g(x) = \exp\left[\sum_{j=1}^{\infty} \varepsilon_j \frac{(-1)^j}{j!} D^j f(x)\right]. \tag{11}$$

In practice, the representation of the serial function is taken as a series with few terms. So, the model adopted is as follows:

$$g(x) \approx \alpha(x)\left(1 + \frac{k_3}{6}H_3(x) + \frac{k_4}{24}H_4(x) + \frac{k_3^2}{72}H_6(x) + \cdots\right)$$

$$G(x) = \int_{-\infty}^{x} g(t)\, dt = \varnothing(x) - \left[\frac{k_3}{6}H_2(x) + \frac{k_4}{24}H_3(x) + \frac{k_3^2}{72}H_5(x) + \cdots\right]\alpha(x) \tag{12}$$

With: x between $-\infty$ and $t + \infty$, $k_3 = (\beta_1)^{1/2}$; $k_4 = \beta_2 - 3$;

$$\alpha(x) = \frac{1}{\sqrt{2\pi}} \exp\left(-\frac{x^2}{2}\right) \quad \text{and} \quad \varnothing(x) = \int_{-\infty}^{x} \alpha(u)\, du$$

$$H_2 = x^2\text{–}1; \quad H_3 = x^3 - 3x; \quad H_4 = x^4 - 6x^2 + 3;$$

$$H_5 = x^5 - 10x^3 + 15x; \quad \text{and} \quad H_6 = x^6 - 15x^4 + 45x^2 - 15$$

This model must verify the following conditions:

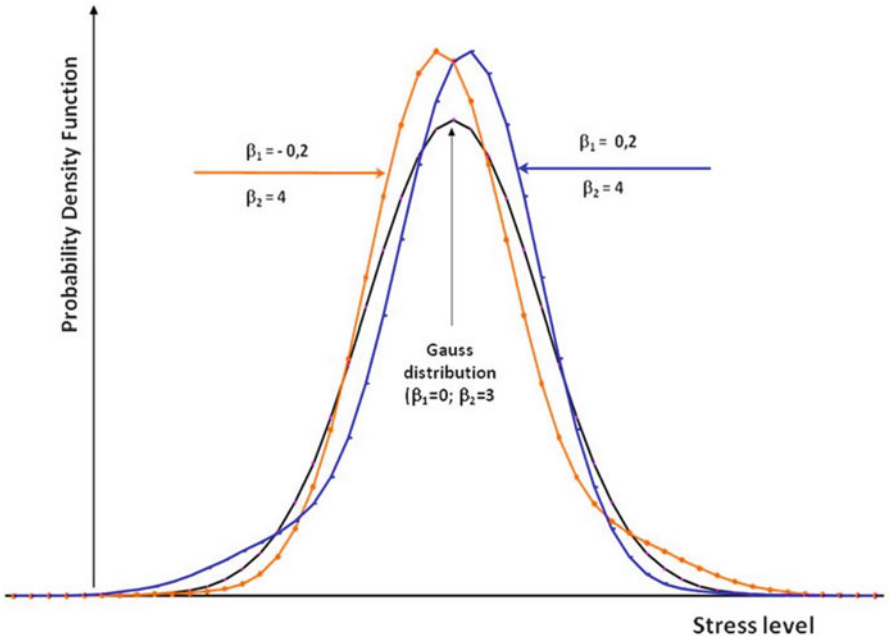

Fig. 18 Results obtained with the GRAM-CHARLIER–EDGEWORTH model

$$\int_{-\infty}^{+\infty} g(x)\,dx=1 \text{ knowing that } \int_{-\infty}^{+\infty} \alpha(x)H_j(x)\,dx=0 \text{ and } g(x)\to 0 \text{ if } x\to\pm\propto$$

The function $f(x)$ taken into account is that of the Gaussian $\alpha(x)$. $H_r(x)$ are the Hermite polynomials. The coefficients k_j depend on the asymmetry and kurtosis which are expressed in terms of different moments μ_r. When $r > 4$, these are known for their unstable nature. For this reason, in practice, the order of development does not exceed the term H_6, and takes into account the terms μ_3 and μ_4. The disadvantage of this model lies in the fact that the model is always defined between $-\infty$ and $+\infty$. For a random variable (Y) which is defined with a mean (m_Y) and a standard deviation (s_Y), any X is obtained by a reduction and centering such that:

$$X = (Y - m_Y)/s_Y. \text{ Thus } m_X = 0 \quad \text{and} \quad s_X = 1.$$

Figure 18 shows different probability densities obtained according to the development of GRAM, CHARLIER, and EDGEWORTH.

2.2 Theoretical Modeling of the Local Events

The statistical models presented in the previous section unknown the intermediate changes in random stress studied. Also to take into account a stress will be represented as a series of ascents and descents. The succession of these changes between peak and trough in the evolution of stresses is another approach to describe the severity of excitatory stress systems and components studied. Thus, modeling is focused on the most representative local events. These are the four families of events (positive peaks, positive trough, negative peaks, and negative troughs) presented in "Counting Local Methods (Local Events)" section. For random stress observed under conditions of use, each type of local events forms a homogeneous sample.

The amplitudes of these four types of events are defined from zero. Thus, the probabilistic modeling of the statistical distribution of these four types of events should consider the following:

- Theoretical model must be defined from zero.
- Upper limit of variation can be considered as infinite because highest amplitudes are much higher than zero.

The statistical distribution model of WEIBULL (Kouta and Play 1999) is used for this kind of phenomenon as the events represent extrema. Appendix 2 presents the technique for estimating the parameters of the WEIBULL distribution for each type of local events. Statistical tests should be performed to ensure the adequacy of proposed laws observed with histograms. Thus, four models of probability density for the four types of local events are obtained. Figure 5 illustrates these four laws of probability.

2.3 Probabilistic Modeling of the Level Crossing

Let $X(t) = \alpha$ level amplitude given, N_α is the number of times this level was exceeded for a small unit of time dt (Rice 1944). $N_\alpha.dt$ is interpreted as the probability that α is exceeded in a time dt, knowing that α may be exceeded if:

$$\alpha - \left|x'(t)\right| dt < x(t) < \alpha \quad x'(t) > 0$$

or

$$\alpha < x(t) < \alpha + \left|x'(t)\right| dt \quad x'(t) < 0 \tag{13}$$

Let $g_{XX'}(u, v)$ the probability density of two random variables $x(t)$ and $x'(t)$ with realizations u and v and

$$g_{XX'}(u, v)\ du\, dv = \text{Prob}\left[(x(t) \in u; u + du) \cap \left(x'(t) \in v; v + dv\right)\right].$$

α crossing probability of is then:

$$N_\alpha \, dt = \int_{-\infty}^{0} dv \int_{\alpha}^{\alpha+|v|dt} g_{xx'}(u,v) \; dv + \int_{0}^{\infty} dv \int_{\alpha-|v|dt}^{\alpha} g_{xx'}(u,v) \; du \tag{14}$$

After integration u and considering infinitesimal dt, then:

$$N_\alpha = \int_{-\infty}^{+\infty} |v| g_{xx'}(\alpha, v) \; dv \tag{15}$$

If we write $g_{XX'}(u,v) = g_{X'/X}(v/x = u)\, g_X(u)$ with $g_{X'/X}(v/x = u)$ the conditional probability $x'(t)$, knowing $x(t) = u$ and $g_X(u)$ the probability density of $x(t)$:

$$N_\alpha = g_x(\alpha) . \int_{-\infty}^{+\infty} |v| \, g_{X'/X}(v/x = \alpha) \; dv = g_x(\alpha) . E\left\{ \left| x' \right| / x = \alpha \right\} \tag{16}$$

In the expression $E\{|x'|/x = \alpha\}$, slope $(|x'(t))|)$ taken into account are those level $x(t) = \alpha$. If this mathematical expectation is calculated for $\alpha = 0$, the number N_0 level 0 crossing is obtained:

$$N_0 = g_x(0) . E\left\{ \left| x' \right| / x = 0 \right\} \tag{17}$$

Similarly, the number of extreme values cannot be modeled but its determination requires the study of curves $(x''(t))$ and zero slopes.

Let $g_{X'X''}(v, w)$, the probability density for two random variables $x'(t)$ and $x'(t)$. Similarly Eqs. (16) and (17)

$$N_e = \int_{-\infty}^{+\infty} |w| g_{x'x''}(0, w) = g_{x'}(0) . E\left\{ \left| x'' \right| / x' = 0 \right\} \tag{18}$$

For a stationary process differentiable (as a differentiable Gaussian process), the cross-correlation function between two successive derivatives of a random variable $x^{(k)}(t)$ and $x^{(k+1)}(t)$ is zero. This has been verified in practice for the majority of studied signals (Osgood 1982).

$$E\left\{ x^{(k)}(t) x^{(k+1)}(t) \right\} = E\left\{ \frac{d^k}{dt^k} x(t) . \frac{d^{k+1}}{dt^{k+1}} x(t) \right\} = E\left\{ \frac{d}{dt} \frac{1}{2} \left[x^{(k)}(t) \right]^2 \right\}$$
$$= \frac{d}{dt} \frac{1}{2} E\left\{ \left[x^k(t) \right]^2 \right\} = \frac{d}{dt} (\text{constant}) = 0.$$

Thus, Eqs. (16), (17), and (18) take a simple form

$$N_\alpha = g_x(\alpha).E\left\{\left|x'\right|\right\} \tag{19}$$

$$N_0 = g_x(0).E\left\{\left|x'\right|\right\} \tag{20}$$

$$N_e = g_{x'}(0).E\left\{\left|x''\right|\right\} \tag{21}$$

These three relationships give theoretical estimates of the number (N_α) of level α crossing, the number of level 0 crossing (N_0), and the number of extreme values (N_e). This evaluation depends on the probability density model adopted for the studied stress on N_α and N_0 and the first derivative of the N_e. These probability densities are weighted by the average slope $E\{|X'|\}$ for N_α and N_0 and the mean curvatures $E\{|x''|\}$ for N_e.

Pearson model (Sect. 2.1.2) or its replacement laws as well as the model of Gram-Charlier–Edgeworth (Sect. 2.1.3) fit well enough to model the probability densities of X and of X' ($g_X(x), g_X(0), g_{X'}(0)$). $E\{|X'|\}$ and $E\{|x''|\}$ are global estimates obtained from a theoretical and only for a Gaussian stress. To make the evaluation of these elements closest to the specificity of each stress studied (Kouta 1994), we must calculate the average slopes and curvatures for each amplitude histogram studied class.

Thus, a more global modeling is defined. It allows an improvement of counting the number of crossings of either a level, either extreme values, or the number of level 0 crossing:

$$N_\alpha(c_k) = g_x(\alpha).E\left\{\left|x'\right|/x \in \left[\alpha - \frac{\Delta c}{2}; \alpha + \frac{\Delta c}{2}\right]\right\} \tag{22}$$

$$N_0(c_{k*}) = g_x(0).E\left\{\left|x'\right|/x \in \left[-\frac{\Delta c}{2}; \frac{\Delta c}{2}\right]\right\} \tag{23}$$

$$N_e(c_k) = g_{x'}(0).E\left\{\left|x''\right|/x' = 0x \in \left[\alpha - \frac{\Delta c}{2}; \alpha + \frac{\Delta c}{2}\right]\right\} \tag{24}$$

With c_k: class k; c_{k*}: class of center containing the amplitude 0; Δc: class width.

Appendix 4 presents the theoretical modeling of the level crossing in the case of a Gaussian stress. The relations Eqs. (22), (23), and (24) are obtained from the probability densities of theoretical (g_X or $g_{X'}$) and the information observed in the studied random stress (average slopes or curvatures amplitude class). Figure 19 (for stress shown in Fig. 10) shows the difference between the counting results of

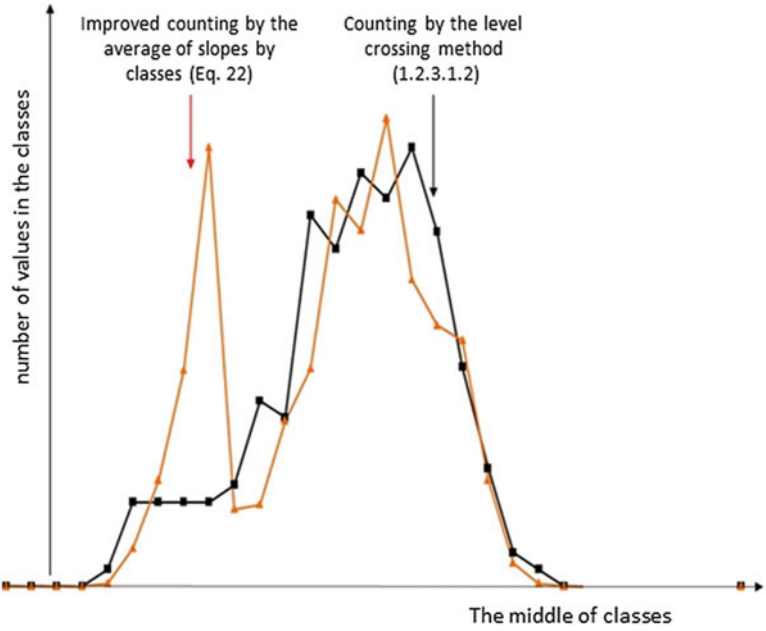

Fig. 19 Comparison of results obtained with different counting methods

numerical level crossings and the results obtained with Eq. (22). In classes of the most negative amplitudes, there are little effective digital values. However, these amplitudes reflect the intensity of the impact when passing over bumps of concrete in this particular case. From the point of view of fatigue of mechanical components, these amplitudes have a significant importance. The product of the number of these amplitudes by the average of their slopes can take into account the effect of these amplitudes.

2.4 Envelope Modeling of a Random Loading

The model of extreme value distribution defines statistics of each extreme group without taking into account their links with the rest of the signal. The objective of this section is to define the probability of exceeding extreme of any level taking into account their statistical distribution and contribution to the dynamics of the signal by taking into account the slopes and curvatures, in the same spirit to that adopted for the development of model exceeded level (2.3).

$f_M(\alpha)d\alpha$ of the probability of occurrence of a maximum at time t with $\alpha < x(t) < \alpha + d\alpha$, this depends on the probability distribution triple $g_{xx'x''}(u, v, w)$ connecting the stress (x), its first derivative (x'), and its second derivative (x''):

$$f_M(\alpha)\ d\alpha.N_{\mathrm{M}}\ dt = \int_{-\infty}^{0}\int_{0}^{|w|dt\alpha+d\alpha}\int_{\alpha} g_{xx'x''}(\alpha,v,w)\ du\ dv\ dw \tag{25}$$

With N_{M}: number of maximum values.

This formulation relates positive extremes. Similarly, the probability of appearance of a minimum (negative extreme) between α and $\alpha + d\alpha$ during dt is $f_m(\alpha)$ $\{=f_M(-\alpha)\}$, an extreme appears in the following conditions:

$$\alpha < x(t) < \alpha + d\alpha, \quad 0 < x'(t) < \left|x''(t)\right| dt \quad \text{and} \quad x''(t) < 0 \ \text{(pics)}$$

Then:

$$f_M(\alpha) = N_{\mathrm{M}}.\int_{-\infty}^{0} |w|\, g_{xx'x''}(\alpha,0,w)\ dw \tag{26}$$

and

$$f_m(\alpha) = N_{\mathrm{m}}\int_{0}^{\infty} |w| g_{xx'x''}(\alpha,0,w)\ dw \tag{27}$$

Appendix 5 presents the modeling of envelope for a Gaussian stress.

2.5 Counting Matrix Methods

These methods include information on slopes and curves observed in a random stress (Rice 1944).

The improved count of level exceeded by the consideration of slope provides a global read of the nature of the severity that the studied mechanical component undergoes during its use. The extreme spectrum response (or strength) presents energy levels depending on the frequencies that constitute the stress studied. The combination of these two types of analysis is done using the two-dimensional representations of transition matrices (Markov, expanses-slopes, and extreme-curvatures). These show the relationship between the local and global behavior. The transition matrix (or Markov) presented in Sect. 1.2.3.2.5 is one of these representations. This representation shows the evolution of the average of expanses in stress studied. For example in the case where the stress is studied stress, the evolution of the average stress influences, in an important way, on the life. Matrices are presented here:

- The matrix expanses-slopes. It gives the number of a given extended for a given slope.
- The matrix extreme-curvatures. It gives the number of an extremum for curvature.

These matrices are built from a clean signal (after grouping into classes of stress). The expanses-slopes matrix is to group different slopes under which a transition occurred between two extreme values. A frequency can be associated with each term of the matrix. Thus, this matrix shows the frequency distribution by type of transition. The matrix connecting the second derivative extrema is to bring together the various extreme amplitudes according to the second derivative or curvature. Figure 20a, b show diagrams of the construction of two matrices. For expanses-slope matrix, the cells of the upper right and the lower ones left are empty because no negative transition can have a positive slope as well as a positive transition can have a negative slope. The top left quarter of the extended-slope matrix (Fig. 20a) shows, from left, the distribution of negative slopes of the largest observed to the lowest. Quarter of the bottom right indicates, always starting from the left, the distribution of positive slopes of the lower to the higher. Thus, the part is on the far left quarter of the top left and the one found on the far right of the bottom right quarter largely explain the severity of stress. Figure 21a shows the matrix for expanses slope the stress of Fig. 10 (Sect. 1). The matrix of extrema-second derivatives (Fig. 21b) provides guidance concerning the regularity or irregularity of the stress studied. Indeed, more the effective of the upper left quarter and the lower ones on the right are important, more the stress is irregular and it contains transitions with nonzero average. A stress has considerable regularity in the case where the top and bottom right quarters of the left have large numbers. Note that the regularity of a stress is synonymous with severity. Stress is regular when it has little or no fluctuation between two successive extrema of opposite signs. Figure 21b shows the matrix of extrema-second derivatives for the stress of Fig. 10, number 5 $(2 + 2 + 1)$, on the top right of the matrix reflects the five major shocks received by the vehicle during its passage over five bumps of concrete.

2.6 Conclusion

Modeling random loads is based on statistical approaches and their interaction with the dynamic behavior of the studied stresses. Statistical approaches include the global approach and local approach. The global statistical modeling leads to a probability distribution that assesses the risk of reach (or exceed) a given amplitude. Local statistical modeling focuses on extreme events of stress studied. Deemed of a random stress to a random path leads probabilistic models which include information and the frequency analysis, in particular, data concerning the speed and acceleration of the stress studied. Now, probabilistic models will help address the fatigue design calculations as well as the definition of laboratory test conditions based on actual conditions of use (Part 3).

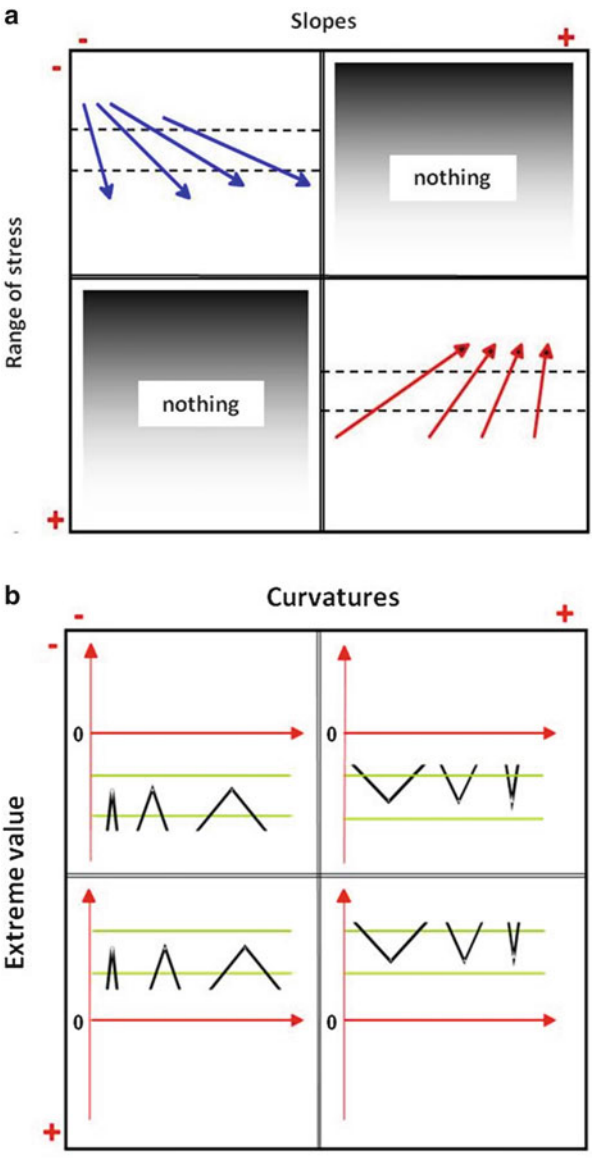

Fig. 20 Construction scheme (**a**) range-slopes matrix and (**b**) extreme-curvatures matrix

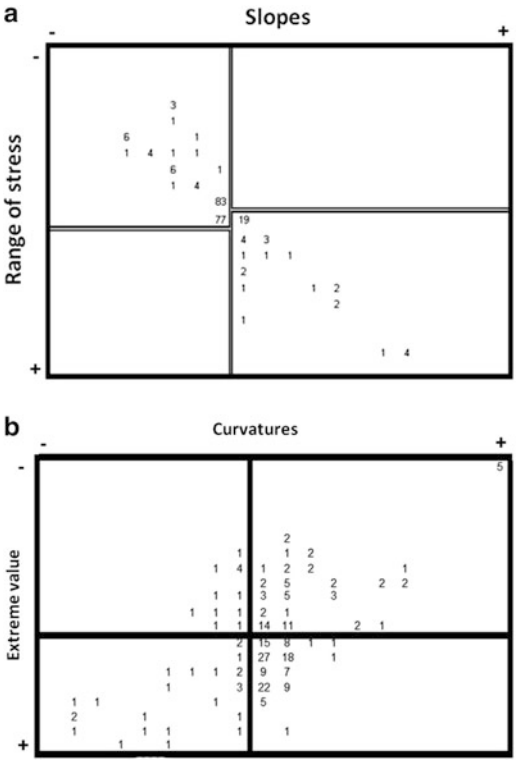

Fig. 21 Example of (**a**) range-slopes matrix and (**b**) extreme-curvatures matrix (stress Fig. 10)

Appendix 1: Main Solutions of the Pearson System and Replacement Laws

Introduction of the Bêta 1 Law

This law takes into account all possible asymmetries between 0 and 1.8. Regarding kurtosis, it takes into account the kurtosis between 1 and at most 5.8. This physically means that this law is limited in its horizontal extension. In fact, this law is theoretically defined on an interval. The standard form of the probability distribution is expressed as follows:

$$f_X(x) = \frac{\gamma\,(p+q)}{\gamma(p)\gamma(q)} x^{p-1}(1-x)^{q-1} \tag{28}$$

with: x between 0 and 1, $\gamma(t) = \int_0^\infty \mathrm{e}^{-u} u^{t-1}\, du$, p and q are the shape parameters of the probability distribution. They are expressed in terms of the mean (m_X) and standard deviation (s_X) of the random variable X.

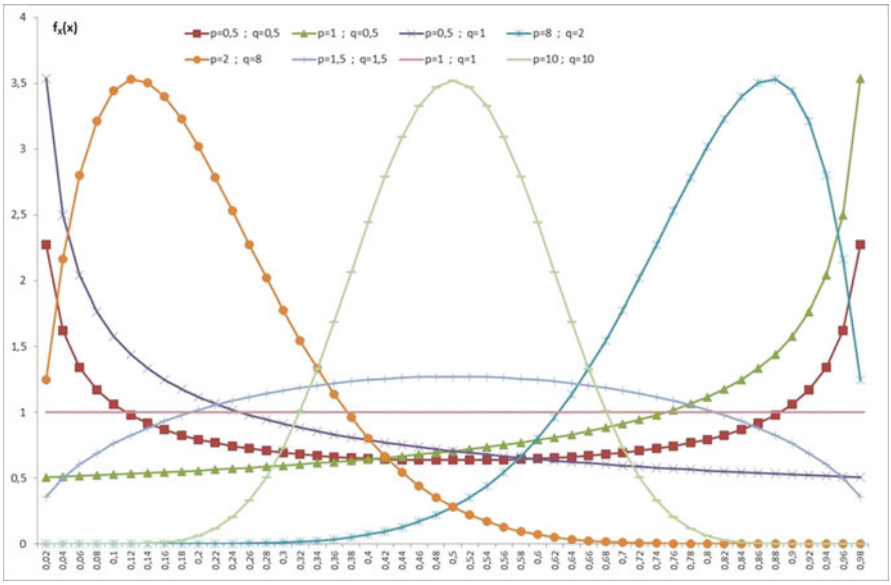

Fig. 22 Probability density function $f_x(x)$ of the Beta 1 law as a function of its parameters

$$p = -m_x + \frac{1 - m_x}{{v_x}^2} \tag{29}$$

$$q = \frac{m_x - 1}{m_x} . \left(m_x + \frac{m_x - 1}{{v_x}^2} \right)$$

with $v_x = s_x / m_x$ coefficient of variation.

For a random variable which is defined between any two terminals (a and b), X is obtained by the following change of variable:

$$X = (Y - a) / (b - a)$$

Thus, $m_X = (m_Y - a)/(b - a)$ and $s_X = s_Y/(b - a)$.

Figure 22 shows different shapes of the probability law in function of p and q. This type of probability distribution is used for random stress that is physically defined between two terminals. Both terminals must be of the same order of magnitude.

Introduction of the Bêta 2 Law

This probability law takes into account the medium and high kurtosis. It also takes into account all possible asymmetries between 0 and 1.8. For these reasons, the law favors Beta 2 promotes kurtosis versus asymmetry. This law is theoretically defined from a low left δ (named offset) and infinity. It is easier to work with the "standard form" of this law. The "standard form" for a probability law which the variable varies between a threshold and infinity is obtained by a change of variable which leads to work with a probability density function which the variable varies between 0 (instead of δ) and infinity. The standard form of the probability distribution is expressed as follows:

$$f_X(x) = \frac{\gamma\,(p+q)}{\gamma(p)\gamma(q)} \frac{x^{p-1}}{(x+1)^{p+q}} \tag{30}$$

with: x is between 0 and ∞.

p and q are the shape parameters of the probability distribution. They are expressed in terms of the mean (m_X) and standard deviation (s_X) of the random variable X.

$$p = m_x + \frac{m_x + 1}{{v_x}^2}$$

and

$$q = 2 + \frac{m_x + 1}{m_x.{v_x}^2} \tag{31}$$

with $v_x = s_x/m_x$.

Figure 23 shows various shapes of the probability law in function of p and q. For this chart, p is 3 and q is between 1 and 6. The variation of p leads only to homotheties on the curves of probability density. This kind of probability distribution is used for random stress which we observe (or we think) that physically dispersion phenomena or kurtosis are more predominant than the phenomena of asymmetry.

In the event that difficulties are encountered when handling this probability law, then it can be replaced by a Log-Normal law which is easier to operate. The standard form of the probability distribution is expressed as follows:

$$f_X(x) = \frac{1}{\sigma\sqrt{2\pi}} \frac{1}{x}.\exp\left(-\frac{1}{2}\left(\frac{\ln(x)-m}{\sigma}\right)^2\right) \tag{32}$$

with: x is between 0 and ∞.

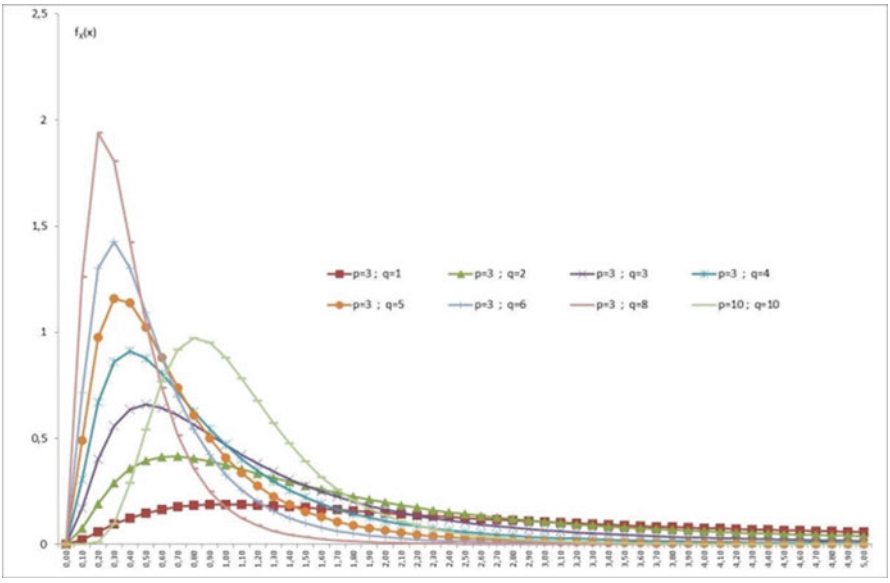

Fig. 23 Probability density function $f_X(x)$ of the Beta 2 law as a function of its parameters

$$m = \ln\left(\frac{m_x}{\sqrt{1+{v_x}^2}}\right) \quad \text{and} \quad \sigma = \sqrt{\ln\left(1+{v_x}^2\right)} \tag{33}$$

For a random variable which is set between the infinite and δ, X is obtained by the following change of variables: $X = (Y - \delta)$. Thus, $m_X = (m_Y - \delta)$ and $s_X = s_Y$. Figure 24 shows the good approximation of the Beta 2 law by Log-Normal law.

Introduction of the Gamma law

According to the abacus of Pearson, the probability distribution is defined in the intermediate zone between Beta 1 law and Beta 2 law. Thus, its contribution is located mainly in consideration of asymmetry and less kurtosis. For this reason, the Gamma law promotes asymmetry versus kurtosis. This law is theoretically defined between a threshold δ and infinity. The standard form of the probability distribution is expressed as follows:

$$f_X(x) = \frac{a^p}{\gamma(p)} x^{p-1}.\exp(-ax) \tag{34}$$

with: x is between 0 and ∞.

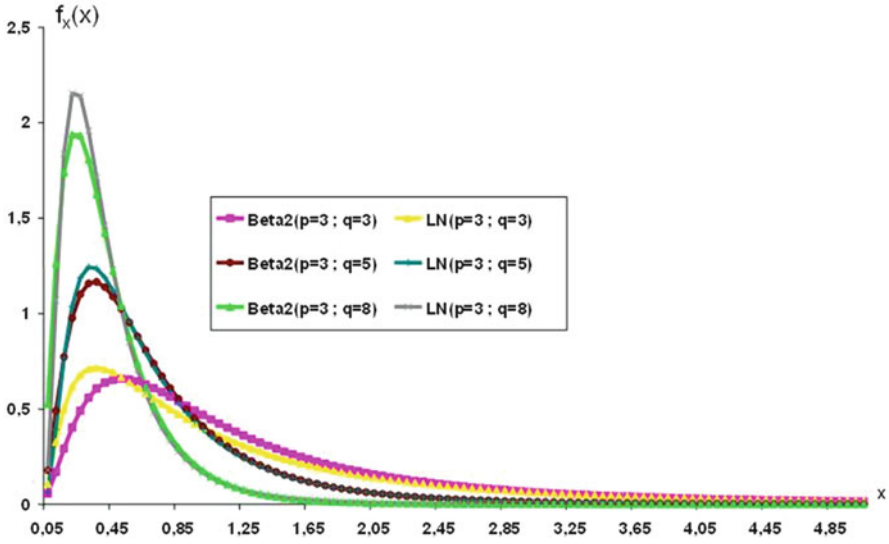

Fig. 24 Comparison between Beta 2 law and Log-Normal

p and q are the shape parameters of the probability distribution. They are expressed in terms of the mean (m_X) and standard deviation (s_X) of the random variable X.

$$p = \frac{1}{{v_x}^2} \quad \text{and} \quad a = \frac{1}{m_x.{v_x}^2} \tag{35}$$

with $v_x = s_x/m_x$.

Figure 25 shows different forms of the probability law function of a and p. For this graph, a is set to 1 and p is between 0.5 and 5. Variation of a led only to homotheties on the probability density curves. This kind of probability law is used for random stress which is observed (or is thought) that physically, the important phenomena of displacement of the medium or of asymmetry that are more predominant kurtosis phenomena.

As for the Beta 2 law, the gamma distribution can be replaced by another law easier to handle and well known is the Weibull distribution. The standard form of this law is expressed as follows:

$$f_X(x) = \frac{\beta}{\eta}\left(\frac{x}{\eta}\right)^{\beta-1} \exp\left\{-\left(\frac{x}{\eta}\right)^{\beta}\right\} \tag{36}$$

with: x is between 0 and ∞.

With the expectation (or mean) and standard deviation, which are expressed as follows:

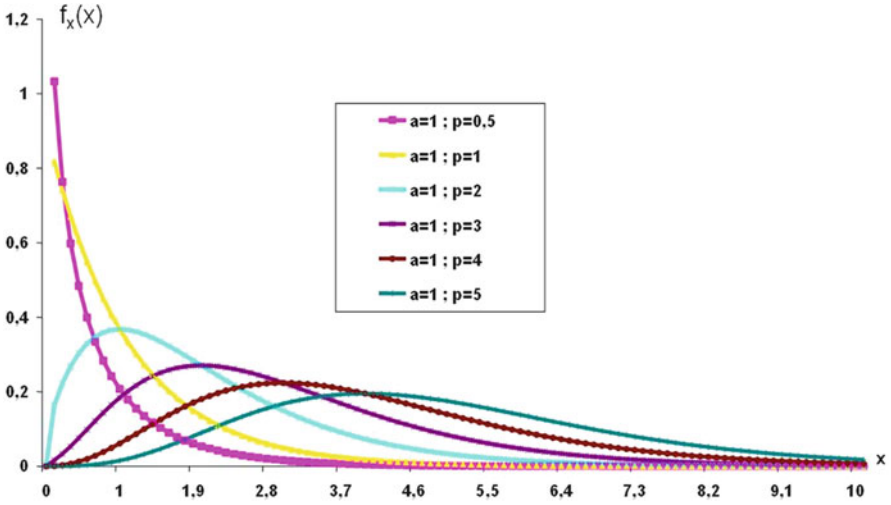

Fig. 25 Probability density function $f_x(x)$ of the Gamma distribution as a function of its parameters

$$E\{X\} = m_X = \eta\gamma\left(1 + \frac{1}{\beta}\right)$$

and

$$s_X = \eta\sqrt{\gamma\left(1 + \frac{2}{\beta}\right) - \left(\gamma\left(1 + \frac{1}{\beta}\right)\right)^2} \tag{37}$$

The β factor is often called form factor η and the scale factor. For a random variable which is set between the infinite and δ, X is obtained by the following change of variable:

$$X = (Y - \delta)\,.\ \text{Thus}\ \ m_X = (m_Y - \delta) \quad \text{and} \quad s_X = s_Y\,.$$

Figure 26 shows the good approximation of Gamma law with a WEIBULL law. Thus, WEIBULL law is the most appropriate model for modeling the random dispersion of mechanical stresses that are defined from a given threshold and that their asymmetry and kurtosis them put in the intermediate zone between the law of the Beta 1 and the Beta 2. In addition, WEIBULL law is easy to handle and estimation of its parameters methods is now well known.

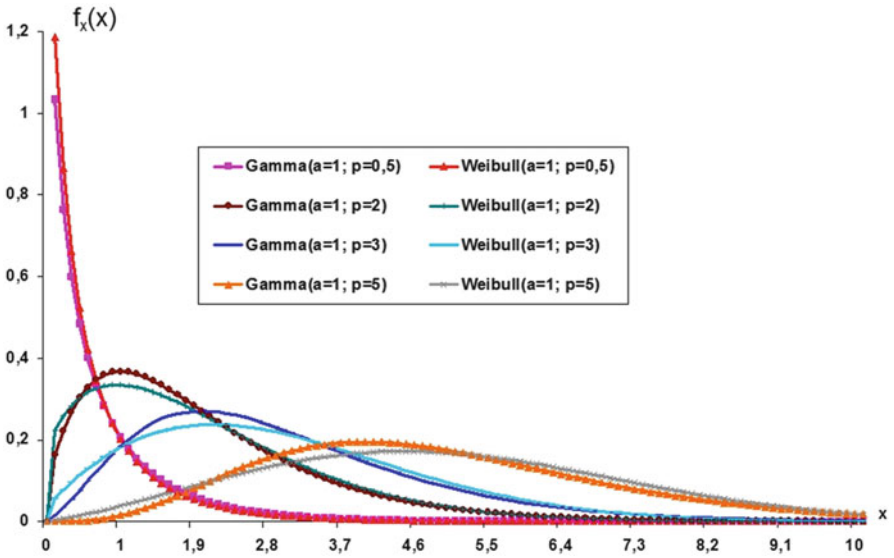

Fig. 26 Comparison between Gamma law and WEILBULL law

Appendix 2: Method of Estimate of the Weibull Law Parameters Around the Four Types of Local Events

The separation of the four types of local events in four samples used to calculate indicators for each sample form: mean $= \overline{x}$, standard deviation $= s_X$, asymmetry $= G_1$ (or β_1), and kurtosis $= G_2$ or (β_2). X, a random variable with Weibull W $(\beta, \eta; \delta = 0)$. The formulation of the probability density function of X, expectation (or its average) and standard deviation are given by the relations Eq. (37) of "Introduction of the Gamma law" of Annex A. Table below gives the theoretical expressions of the dispersion coefficient (v_X), of the asymmetry G_1 and of the kurtosis G_2 the Weibull distribution. These formulas are expressed exclusively in terms of the form factor of the distribution (β).

$$v_x = \frac{s_x}{m_x} = \frac{\left(\gamma_2 - (\gamma_1)^2\right)^{1/2}}{(\gamma_1)}$$

$$G_1 = \frac{\gamma_3 - 3\gamma_2\gamma_1 + 2(\gamma_1)^3}{\left(\gamma_2 - (\gamma_1)^2\right)^{3/2}}$$

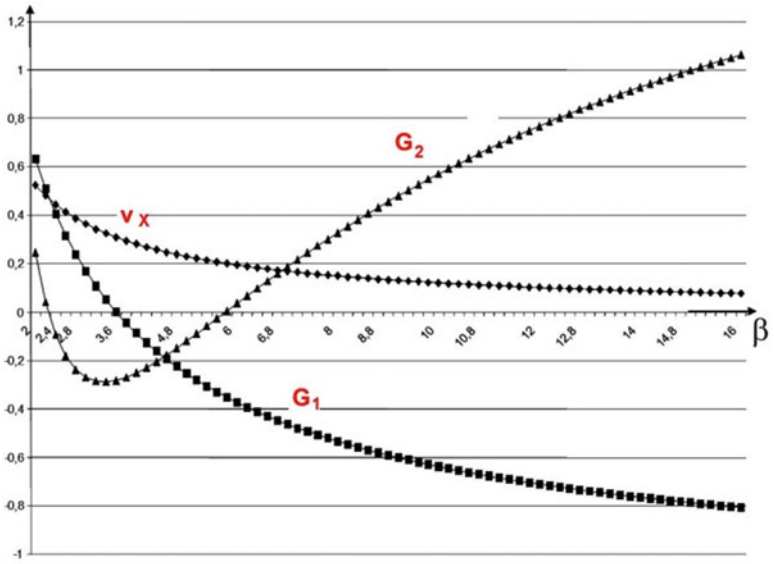

Fig. 27 Evolution of v_X, G_1 and G_2 of the law the Weibull based on shape factor parameters β

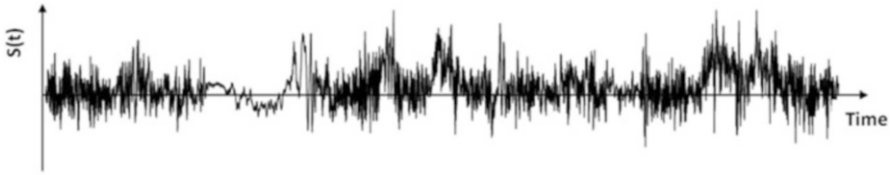

Fig. 28 Viewing the input torque to the front stabilizer bar of a motor vehicle

$$G_2 = \frac{\gamma_4 - 3\gamma_3\gamma_1 - 3(\gamma_2)^2 + 12\gamma_2(\gamma_1)^2 - 6(\gamma_1)^4}{\left(\gamma_2 - (\gamma_1)^2\right)^2} \tag{38}$$

with $\gamma_r = \gamma\left(1 + \frac{r}{\beta}\right)$.

Thus, the shape factor may be obtained β by inverting one of three functions v_x, G_1, or G_2. Figure 27 shows the theoretical evolution of v_x, G_1, and G_2. According to β which the $v_X = F_1(\beta)$, $G_1 = F_2(\beta)$, and $G_2 = F_3(\beta)$. Given the shape of the last three functions, the easiest way is to reverse (a numerical method) function G_1. Figure 28 shows a random stress representing the couple in an industrial vehicle stabilizer bar when passing over a poorly maintained road. The recording time is 5 min.

Table 4 Parameters of Weibull laws

Parameter	G_1	β
Peak > 0	1.25	1.36
Hollow < 0	0.812	1.76
Peak < 0	0.925	1.63
Hollow > 0	1.686	1.12

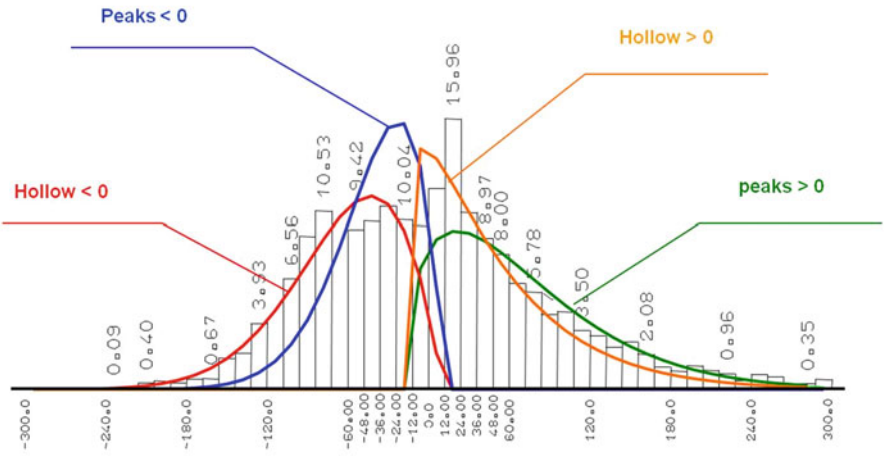

Fig. 29 Histograms peaks > 0 and hollow < 0 and probability distributions of four local events

Table 4 presents the values obtained for the different parameters of Weibull laws for the four types of local events. Figure 29 shows the adequacy of the proposed relationship with histograms experimentally observed laws.

Appendix 3: Extrem Response Spectrum for a Random Loading

Extrem response ER is calculated from the maximum met once during the excitation time response. For recording a duration T, the total number of peaks above $z0$ is given by

$$N = N_e T F_M(u_0) \tag{39}$$

With $F_M(u) =$ cumulative probability function given in E3 of Annex E and N_e is the number of extreme values.

The largest peak for the duration T (on average) approximately corresponds to u_0 level that is exceeded only once, hence:

$$F_M\,(u_0) = 1/\,(N_e T) \tag{40}$$

The level u_0 is determined by successive iterations. Distribution $F_M(u)$ is a decreasing function of u. We consider two values u, such that:

$$F_M\,(u_1) < F_M\,(u_0) < F_M\,(u_2) \tag{41}$$

and, at each iteration, the interval is reduced (u_1, u_2) until, for example:

$$\frac{F_M\,(u_1) - F_M\,(u_2)}{F_M\,(u_0)} \prec 10^{-2} \tag{42}$$

Hence extrapolation:

$$z_m \approx z_0 = (V(X))^{1/2} \left\{ [u_2 - u_1] \frac{F_M\,(u_1) - F_M\,(u_2)}{F_M\,(u_0)} + u_1 \right\} \tag{43}$$

and $\mathrm{ER} = (2\pi f_0)^2 Z_m$.

With the same assumptions, the average number of threshold exceedances $z = \alpha$ response with positive slope during a recording period T for stress a Gaussian is given by the relationship:

$$N_\alpha^+ = TN_\alpha = TN_0 \exp\left(-\frac{\alpha^2}{2\sqrt{V(X)}}\right) \quad \text{and} \quad N_0 = \frac{1}{\pi}\sqrt{\frac{V\,(x')}{V(x)}} \tag{44}$$

Considering that the threshold α is exceeded only once, is obtained by $N_\alpha^+ = 1$

$$\alpha = \sqrt{2V(X)\ln\,(N_0 T)}$$

Whence

$$\mathrm{ER} = 4\pi^2 f_0^2 \sqrt{2V(X)\ln\,(N_0 T)} \tag{45}$$

In the case of a random stress whose PSD is represented by several levels ($G_i = \Phi$ cf. Sect. 1) each of which is defined between two frequencies f_i et f_{i+1}, the various components of ER are obtained as follows:

$$V(X) = \int_0^\infty G(f).df = \frac{1}{(2\pi)^4.f_0^3}\frac{\pi}{4.\xi}\sum_i G_i\,.\,[I_0\,(h_i + 1) - I_0\,(h_i)] \tag{46}$$

$$V\left(\dot{X}\right) = (2\pi)^2.\int_0^\infty f^2.G(f).df = \frac{1}{(2\pi)^2.f_0}\frac{\pi}{4.\xi}\sum_i G_i.\left[I_2\left(h_i+1\right) - I_2\left(h_i\right)\right] \tag{47}$$

$$V\left(\ddot{X}\right) = (2\pi)^4.\int_0^\infty f^4.G(f).df = f_0.\frac{\pi}{4.\xi}\sum_i G_i.\left[I_4\left(h_i+1\right) - I_4\left(h_i\right)\right] \tag{48}$$

with $G(f) = |H(f)|^2.G_{\ddot{x}}(f)$, $h_i = f_i/f_0$ and $h_{i+1} = f_{i+1}/f_0$.

$$I_0 = \frac{\xi}{\pi.\alpha}.\ln\left(\frac{h^2+\alpha h+1}{h^2-\alpha h+1}\right) + \frac{1}{\pi}.\left[\text{Arctan}\left(\frac{2.h+\alpha}{2.\xi}\right) + \text{Arctan}\left(\frac{2.h-\alpha}{2.\xi}\right)\right] \tag{49}$$

$$I_2 = -\frac{\xi}{\pi.\alpha}.\ln\left(\frac{h^2+\alpha h+1}{h^2-\alpha h+1}\right) + \frac{1}{\pi}.\left[\text{Arctan}\left(\frac{2.h+\alpha}{2.\xi}\right) + \text{Arctan}\left(\frac{2.h-\alpha}{2.\xi}\right)\right] \tag{50}$$

$$I_4 = \frac{4.\xi}{\pi}.h + \beta.I_2 - I_0 \tag{51}$$

$$\alpha = 2.\sqrt{1-\xi^2}; \quad \beta = 2\left(1-2.\xi^2\right); \quad Q = 1/\left(2.\xi\right) \tag{52}$$

with $\xi =$ damping factor

Thus:

$$N_e = \frac{1}{\pi}\sqrt{\frac{V\left(x''\right)}{V\left(x'\right)}}, \quad N_0 = \frac{1}{\pi}\sqrt{\frac{V\left(x'\right)}{V(x)}} \quad \text{and} \quad I = \frac{N_0}{N_e} \tag{53}$$

In cases where the statistical distribution of peaks (trough respectively) is modeled by a Weibull law $W(\beta, \eta, \delta)$ with β: shape factor, η; scale parameter and δ: shift (often close to zero), we seeks probability $\pi_M(u_0)$ exceeds a maximum for any level u_0 of the amplitude of the response. $\pi_M(u_0) = 1 - F_M(u_0)$ with:

$$F_M\left(U_0\right) = \int_{-\infty}^{u_0} p(u)\, du$$

and over a period of observation T, the mean number of peaks is greater than u_0 always $N = n_p^+ . T\pi(u_0)$. When $N = 1$, the corresponding level is defined by $\pi(u_0) = 1/(n_p^+ . T)$.
with

$$\pi\,(u_0) = \exp\left(-\left(\frac{u_0}{\eta}\right)^{\beta}\right)$$

and knowing the value of n_p^+, it has

$$u_0 = \eta.\left[\ln\left(\frac{\ddot{Z}_{\text{eff}}.T}{2\pi.\dot{Z}_{\text{eff}}}\right)\right]^{1/\beta} \tag{54}$$

While the extrem response becomes

$$\text{ER} = (2\pi.f_0)^2.\eta.\left[\ln\left(\frac{\ddot{Z}_{\text{eff}}.T}{2\pi.\dot{Z}_{\text{eff}}}\right)\right]^{1/\beta} \tag{55}$$

Appendix 4: Theoretical Modeling of the Overrun of Level for a Gaussian Loading

In the Gaussian case, $x(t)$, $x'(t)$, and $x''(t)$ are Gaussian random variables with three densities as successive probabilities:

$$g_x(u) = \frac{1}{\sqrt{2\pi V(x)}}.\exp\left\{-\frac{u^2}{2V(x)}\right\} \tag{56}$$

$$g_{x'}(v) = \frac{1}{\sqrt{2\pi V\,(x')}}.\exp\left\{-\frac{v^2}{2V\,(x')}\right\} \tag{57}$$

$$g_{x''}(w) = \frac{1}{\sqrt{2\pi V\,(x'')}}.\exp\left\{-\frac{w^2}{2V\,(x'')}\right\} \tag{58}$$

Thus, we have:

$$E\left\{\left|x'\right|\right\} = \int_{-\infty}^{+\infty} |v|\, g_{x'}(v)\; dv = \sqrt{\frac{2}{\pi}V\,(x')} \tag{59}$$

$$E\left\{\left|x''\right|\right\} = \int_{-\infty}^{+\infty} |w| g_{x''}(w)\, dw = \sqrt{\frac{2}{\pi} V\left(x''\right)} \tag{60}$$

Thus, in the case of a Gaussian process, Eqs. (19), (20), and (21) can be written

$$N_\alpha = \frac{1}{\pi}\sqrt{\frac{V\left(x'\right)}{V(x)}}.\exp\left\{-\frac{1}{2}\frac{\alpha^2}{V(x)}\right\} \tag{61}$$

$$N_0 = \frac{1}{\pi}\sqrt{\frac{V\left(x'\right)}{V(x)}} \tag{62}$$

$$N_e = \frac{1}{\pi}\sqrt{\frac{V\left(x''\right)}{V\left(x'\right)}} \tag{63}$$

Hence expression of Gaussian irregularity factor

$$I_g = \frac{N_0}{N_e} = \frac{V\left(x'\right)}{\sqrt{V(x)V\left(x''\right)}} \tag{64}$$

From this factor, the factor ε is defined as the bandwidth of the studied process. The last (as I and I_g) is between 0 and 1.

Bandwidth is expressed by the number of zero crossings by increasing values N_0 and the number of local maxima N_e (positive or negative) of the observation time. We put:

$$\varepsilon = \sqrt{1 - I_g^2} \tag{65}$$

Notes:

1. The relation Eq. (65) is a definition and simply reflects the fact that, when a process narrowband $N_0 = N_e$ (see Fig. 11a) and therefore $\varepsilon = 0$, and when a broadband process (Fig. 11b) $N_e > N_0$, where $N_e \gg N_0$ $\varepsilon \to 1$.
2. When $\varepsilon = 0$, in the case of a trajectory narrowband cycle thinking has a precise meaning, since $N_0 = N_e$.
3. When $\varepsilon = 1$, the notion of cycle is likely to various interpretations, the definition of "number of cycles" depends on the counting method.

Appendix 5: Envelope Modeling for a Gaussian Loading

For a Gaussian trajectory, correlation coefficient between the signal $x(t)$ and its first derivative $x'(t)$ is zero. As follows:

$$g_{XX'X''}(u,v,w) = g_{X'}(v)\, g_{XX''}(u,w)$$

Dual distribution $g_{xx''}(u,w)$ between the signal and its second derivative is expressed in a bi-normal distribution:

$$g_{xx''}(u,w) = \frac{1}{2\pi\sqrt{k}} \exp\left[-\frac{1}{2k}\left\{V\left(x''\right)u^2 + 2V\left(x'\right)uw + V(x)w^2\right\}\right] \quad (66)$$

with $k = V(x)V(x'') - [V(x')]^2$

The probability density peaks (Eq. (26)) to be written:

$$f_M(\alpha) = \text{Prob}\left(\alpha < \text{Max} \le \alpha + d\alpha\right) =$$
$$= \frac{\sqrt{1-I_g^2}}{\sqrt{2\pi}}.\exp\left(-\frac{u^2}{2\left(1-I_g^2\right)}\right) + \frac{I_g u}{2}\exp\left(-\frac{u^2}{2}\right)\left[1 + \text{erf}\left(\frac{I_g u}{\sqrt{2\left(1-I_g^2\right)}}\right)\right] \quad (67)$$

And the cumulative probability function is:

$$F_M(\alpha) = \text{Prob}\left(\text{Max} \le \alpha\right)$$
$$= \frac{1}{2}\left\{1 - \text{erf}\left(\frac{u}{\sqrt{2\left(1-I_g^2\right)}}\right)\right\} + \frac{I_g}{2}\exp\left(-\frac{u^2}{2}\right)\left\{1 + \text{erf}\left(\frac{I_g u}{\sqrt{2\left(1-I_g^2\right)}}\right)\right\} \quad (68)$$

with $I_g = \frac{V(X')}{\sqrt{V(X)V(X'')}}$ Gaussian irregularity factor,

$$u = \frac{\alpha}{\sqrt{V(X)}} \quad \text{and} \quad \text{erf}(x) = \frac{2}{\sqrt{\pi}}\int_0^x e^{-\lambda^2/2}\, d\lambda.$$

For $I_g \approx 1$ ($\varepsilon = 0$, stress narrowband), probability density becomes: $f_M(\alpha; I_g) \approx u.\exp(-u^2/2)$. This approximation corresponds to the Rayleigh distribution. Thus, we find that for a narrowband random stress, the distribution of maximum values follow a Weibull distribution with shape factors of individual $\beta = 2$; $\eta = \sqrt{2V(x)}$; $\delta \ge 0$.

The influence of three main variances $V(x)V(x')$ and $V(x'')$ is studied on the distribution of extreme values. This influence is observed through the irregularity factor I_g. The difficulty of this study lies in the fact that evolutions of x, x', and x'' are interdependent for a random trajectory.

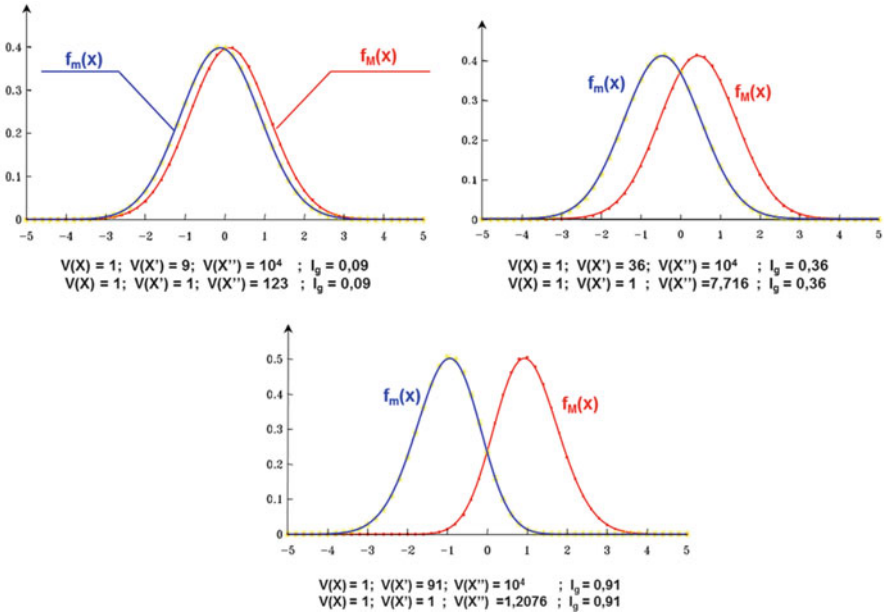

Fig. 30 Influence of the variance of the first derived and second derived on the modeling of the envelope

To simplify the presentation, consider the assumption of a variance $V(x) = 1$. Figure 30 shows the evolution of the extreme value distribution based on the irregularity factor I_g. The latter is directly proportional to $V(x')$. Increasing this variance is due to the appearance of a variety of slopes increasingly important in the stress. This results in a greater probability of observing extreme values t_o higher levels of amplitudes and conversely lower probability amplitudes of fluctuations around the middle of the path. Thus, the distribution of positive extreme and negative extreme deviate from each other in the growth of the irregularity or the variance factor of the second derivative. Significant dispersion of the variance of the curves or the second derivative ($V(x'')$) indicates an occurrence of a wide variety of shapes for the peaks and ridges on the random path. This dispersion occurs in all classes of amplitudes, where a large irregularity (I_g decreases). I_g is inversely proportional to $V(x'')$.

Study of the Random Loading Impact

Predictive calculating of the lifetime of a system or component mechanical, operating in real conditions of use, is made from the fatigue of the materials of the components studied.

Material fatigue occurs whenever the efforts and stress vary over time. These random stresses take very different looks (see Sects. 1 and 2). The rupture may well occur with relatively low stress, sometimes less than a conventional limit called "endurance limit" S_D.

Material fatigue is approached in two ways.

The first is based on a global approach where the material is considered as a homogeneous medium at a macroscopic scale. The mechanical properties of the material are presented by the curves of fatigue; the most famous is the "Wöhler." The critical points of the components are defined by the points of the most damaging stress, and lifetime calculations are made at these points.

The second approach to material fatigue based on a local approach which characteristics are considered potential material defects (cracks). In these areas, the stresses lead to the definition of a cracking speed and is obtained when the out of crack length limit is reached.

These two approaches to the calculation of the fatigue lifetime of the systems or mechanical components use the same distributions of random loads.

The presentation of this part will be limited to the global approach because this approach for the strength of materials is widespread and based on a broad competence in the industry. A significant gain in the quality of forecasts is then expected with the inclusion of random stress. Note, however, that the second approach is not excluded and that all developments presented here can be extrapolated.

Principle of Predictive Calculating

Predictive calculating of the lifetime of a system or component mechanical, operating in real conditions of use, is made from four elements:

- Knowledge of load (or stress) it undergoes (Fig. 31a, b). Figure 31a shows the definition of measurement points over time (with predefined pace of time constant Δt). Figure 31b can recall the quantities considered thereafter.
- An endurance law (often based on the Wöhler) (Fig. 31c). Tests conducted for an average stress S_m^0 zero and a stress S_a give results with different numbers of cycles to failure. The distribution is represented by a sequence of points. The different values of stresses are considered. Thereafter, the three curves can be derived with, respectively, $p_r = 50\ \%$, p_0, and $1 - p_0$ of failure probability. Typically, p_0 is between 1 and 10 %.
- A fatigue requirement that sets the limit resistance (Fig. 31d). When the mean stress is not zero, the fatigue limit S_D depends on the value of the mean stress S_m, different models can then be used according to the stress S_m between 0 and R_E or R_m.
- A law of accumulation of damage to account for all the stresses applied to the system or component. Generally, it is the law that is used Miner.

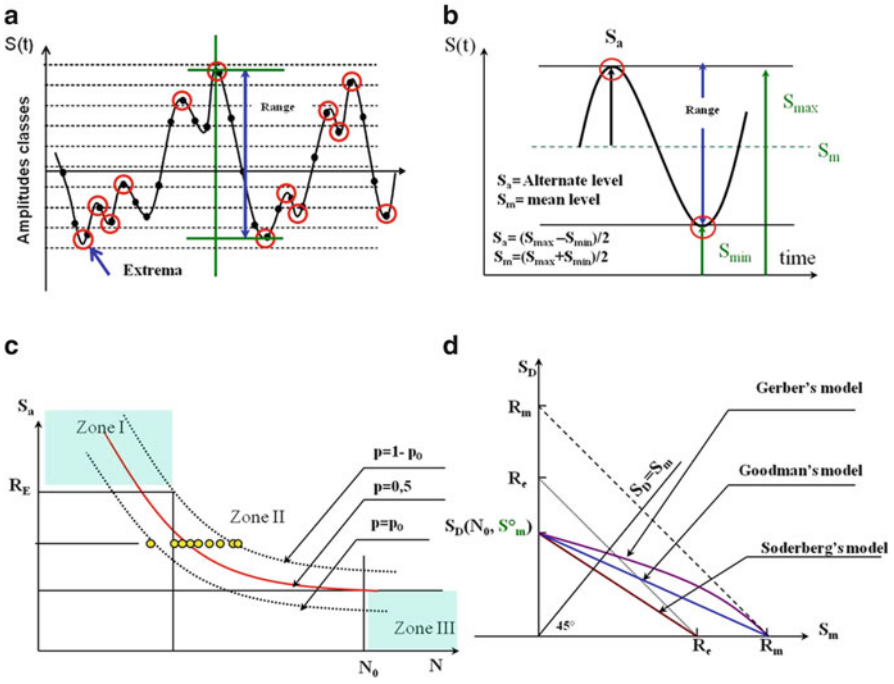

Fig. 31 The four steps of predicting of the lifetime. (**a**) Random stress, (**b**) after counting, (**c**) probabilized Wöhler's curve, (**d**) fatigue criteria

Fatigue and Damage in the Lifetime Validation of a Mechanical Component

The results of the analysis of the stresses measured under actual conditions of use should be exploitable by the steps of the method of calculating the lifetime. Thus, we must find (Sect. 1) counting method for identifying a "statistical load event" in a random loading history. For example, the event may consist of amplitudes of grouped into classes, the extrema, stretches or "cycles" of the stress studied. Often, they are extended or stress cycles which are operated to perform the calculation of a lifetime.

To strengthen the capacity of prediction, calculation of lifetime must have a probabilistic approach to announce reliability. Rather than events or extended cycle type, the load events are grouped into classes where these are the extrema which are better suited to probabilistic modeling (Sect. 2).

Endurance Law or Wöhler Curve

A Wöhler curve (Fig. 31c) represents a probability p to rupture, the magnitude of the cyclic stress ((S_a) considered average for a given stress S_m) based on the lifetime N. Also known as curve S–N (Stress–Number of cycles).

The test conditions must be fully specified in both the test environment and the types of stress applied. Rupture occurs for a number of cycles increases when the stress decreases.

There are *several models of these* curves according to an endurance limit implicitly or explicitly appears. Indeed, when a material is subjected to low-amplitude cyclic stress, fatigue damage can occur for large numbers of cycles. Points of the curve of Wöhler are obtained with the results of fatigue tests on specimens subjected to cyclic loading of constant amplitude.

The curve is determined from which each batch of sample is subjected to a periodic stress maximum amplitude S_a and constant frequency, the failure occurring after a number of cycles N. Each sample corresponds to a point in the plane (S_a, N).

The *results of the fatigue tests* are randomly distributed, such that one can define curves corresponding to given failure probabilities according to the amplitude and the number of stress cycles.

This finding requires the construction of a model to the median ($p_r = 0.5$, 50 % of failures) observed lifetimes, curves at p_0 and at $(1 - p_0)$ are then deducted p_0 is often taken equal to 0.01 (1 % of failures). These curves are called the Wöhler curves probabilized.

Wöhler curves are generally broken down *into three distinct areas* (Fig. 31c):

- Area I: Area of *oligocyclic plastic fatigue*, which corresponds to the higher stresses above the elastic limit R_E of the material. Breaking occurs after a small number of cycles typically varying from one cycle to about 10^5 cycles.
- Area II: Area *of fatigue or limited endurance*, where the break is reached after a limited number of cycles (between 10^5 and 10^7 cycles).
- Area III: Area *of endurance unlimited or safety area* under low stress, for which the break does not occur after a given number of cycles (10^7 and even 10^{10}), higher the lifetime considered for the part.

In many cases, *an asymptotic horizontal branch* to the curve of Wöhler can be traced: the asymptote is called endurance limit or fatigue limit and denoted S_D. The latter is defined at zero mean stress ($S_m^0 = 0$) and corresponds to a lifetime N_0 ($N_0 = 10^7$ cycles often).

In other cases, a conventional endurance limit may be set for example to 10^7 cycles.

Generally, you must use a model that approximates the curves to perform further calculations. Various expressions have been proposed to account for the shape of the curve of Wöhler (Lieurade 1980b). The most practical was proposed by Basquin and she wrote as follows:

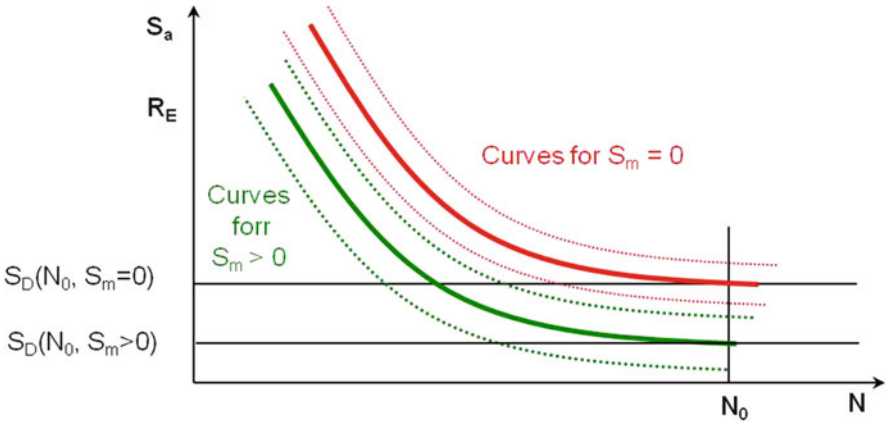

Fig. 32 Influence of mean stress on the network Wöhler curves

$$NS^b = C_1 \tag{69}$$

and

$$\log N + b \log S = C \ (C = \log (C_1)) \tag{70}$$

With $N =$ number of cycles, $S =$ amplitude of the stress, $b =$ slope of the line depends on the material, $C =$ constant dependent right material and the average of the alternating stress fatigue test performed.

In the following text, the coefficient C will be used.

Fatigue tests are usually long term and it is rare to have the results of experiments conducted with a nonzero mean stress.

The increase in mean stress causes a reduction of the lifetime: a network of Wöhler curves can be thought (Fig. 32). Thus, the endurance limit for a chosen number of cycles (e.g., to $N_0 = 10^7$ cycles) decreases. Then, for each nonzero average stress, an endurance limit should be determined. Lacking often experimental results, the calculation is based on a relationship called "fatigue requirement."

Fatigue Requirements

A fatigue test is a threshold defined by a mathematical expression for a fixed lifetime (N_0) and a given material. The threshold separates the state where the part is operating in the state where it is damaged by fatigue.

In general, a fatigue test was developed for cyclic loading with constant amplitude.

It is a relationship between the evolution of the Wöhler curve and the average stress considered. Figure 31d shows the main criteria of fatigue. These graphs are built with a lifetime N_0 (often given as 10^7 cycles) and a given probability of failure ($p_r = 0.5$, 0.1, and 0.01). These different models are (Rabbe et al. 2000b):

$$\text{Goodman model} \quad S_D = S_D^* . \left(1 - \frac{S_m}{R_m}\right) \tag{71}$$

$$\text{Soderberg model} \quad S_D = S_D^* . \left(1 - \frac{S_m}{R_E}\right) \tag{72}$$

$$\text{Gerbermodel} \quad S_D = S_D^* . \left(1 - \left(\frac{S_m}{R_m}\right)^2\right) \tag{73}$$

With $S_D^* = S_D(S_m^0 = 0; N_0)$ endurance limit defined for zero mean stress and number of cycles N_0 selected.

Then, for a given cycle (amplitude, a range) having a nonzero mean, these relationships allow to obtain approximate the endurance limit for the average stress.

Calculation of Fatigue Damage, of Damage Accumulation, and of Lifetime

The concept of damage represents the state of degradation of the material in question. This condition results in a quantitative representation of the endurance of materials subjected to various loading histories.

A law of accumulative damage is a rule to accumulate damage variable D (also called "damage D"), itself defined by a law of damage.

As for the lifetime is defined by a number of cycles N which leads to breakage.

Thus, the application of n cycles ($n < N$) causes a partial deterioration of the treated piece to the calculation. The assessment of damage at a given time is crucial to assess the remaining capacity of lifetime.

Fatemi and Yang (Fatemi and Yang 1998) identified in the literature more than 50 laws of accumulated damage. The most commonly used today is the law of linear cumulative damage to Palmgren–Miner remains the best compromise between ease of implementation and the quality of predictions for large lifetimes (Banvillet 2001). Miner's rule is as follows:

$$d_i = \frac{n_i}{N_i} \tag{74}$$

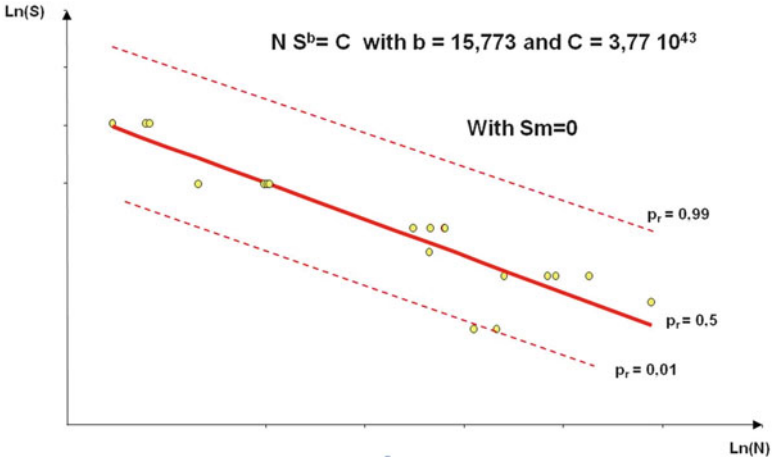

Fig. 33 Basquin Model of the Wöhler curve for Steel A42FP (from Leluan (1992b))

With n_i = the number of repetitions of a given cycle (with amplitude or extended), N_i = the number of repetitions of the same cycle necessary to declare the failed component ($n_i < N_i$).

For different cycles of random stress studied, the global damage is obtained by linear addition of the elementary damage:

$$D = \sum_i d_i = \sum_i \frac{n_i}{N_i} \tag{75}$$

Fracture occurs when D is 1. The lifetime is equal to $1/D$.

Introductory Examples

The different steps of the calculation will be presented with a A42FP case (Leluan 1992b) steel. Figure 33 shows the model Basquin concerning fatigue tests on this steel with alternating stresses whose average is zero. Figure 34 shows the various criteria of fatigue such as steel. An endurance limit calculated from the right Soderberg is lower than those obtained with the right Goodman and the parabola of Gerber.

This difference between endurance limits calculated using criteria of fatigue leads to some significant differences on the calculated life.

Example 1 The first question in this introductory example is how to calculate the damage suffered by the steel A42FP subjected to a stress of 10^{75} cycles, the alternating stress (S_a) is 180 MPa, and mean stress (S_m) of 100 MPa, calculating with a failure probability of 0.5. The second question is to determine the number of repetitions of this stress must be applied for failure:

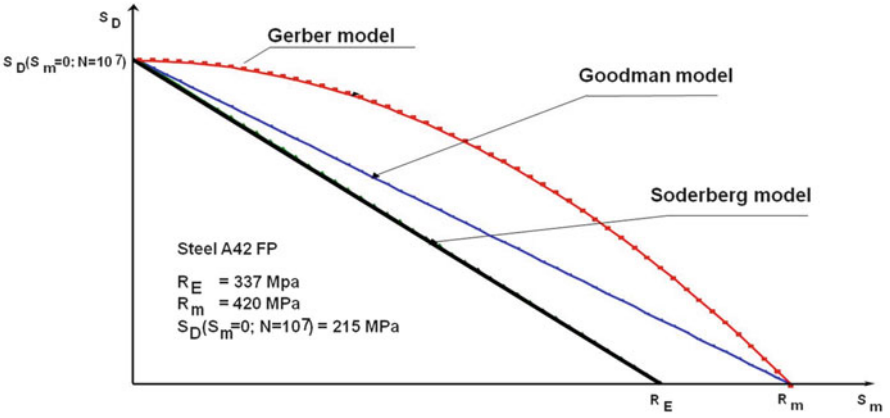

Fig. 34 Criteria of fatigue for Steel A42FP

Step 1: Calculation of the new endurance limit, according to each criteria of fatigue:

Criteria of fatigue	S_D ($S_m = 100$ MPa; $N = 10^7$)
Gerber parabola	203 MPa
Goodman right	164 MPa
Soderberg right	151 MPa

Step 2: Calculation of the new constant C in the model Basquin:

Criteria of fatigue	$C(S_m = 100 \text{ MPa}; S_D) = N \times (S_D)^b = 10^7 (S_D)^b$
Gerber parabola	2.45×10^{43}
Goodman right	8.45×10^{41}
Soderberg right	2.39×10^{41}

Step 3: Calculation of the number of cycles to failure for the stress studied according to the criteria of fatigue. In this case, the calculation is performed at 50 % of probability of failure:

Criteria of fatigue	$N = C \times (S_a)^b$
Gerber parabola	9.15×10^{78}
Goodman right	3.16×10^{77}
Soderberg right	8.93×10^{76}

Step 4: Calculation of damage due to studied stress and the lifetime expectancy. Determination of the number of repetitions to reach failure

Criteria of fatigue	$D = n/N = 10^{75}/N$	Lifetime[a] $= 1/D$
Gerber parabola	1.093×10^{-4}	9,150 times
Goodman right	3.16×10^{-3}	316
Soderberg right	1.12×10^{-2}	89

[a]This result means that the stress will be able to repeat before reaching failure = number of repetitions.

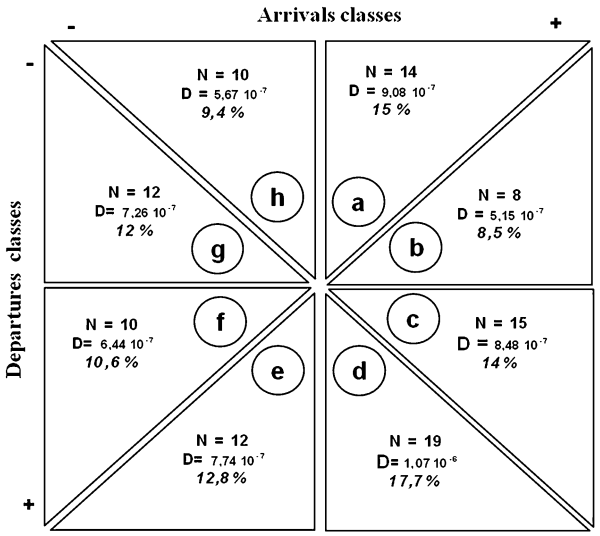

Fig. 35 Distribution of damage per area of the Markov matrix (stress shown in Fig. 10, part 1)

In the case of multilevel constraints, these four steps of calculation (Example 1) are applied for each level and the total damage is obtained according to the rules of linear cumulative damage Miner.

Example 2 It involves the stress of an axle front right of the vehicle. Figure 35 shows the distribution of damage per area of the Markov matrix for stress shown in Fig. 10 (Kouta and Play 2007a). The total damage is 6.05 E-06 and the number of repetitions of this stress before reaching failure is 165,273 times. The separation of Fig. 35 in eight zones ((a)–(h)) allows to visualize the contribution of the elementary stresses.

The nature of the stresses together in each area specified in Fig. 9. Fifteen percent of damage in the area (a) of Fig. 35 can be explained mainly by effective stress that are at the end of the Markov matrix (top right of Fig. 10).

Among a workforce of $N = 15$, a workforce of 5 $(2 + 2 + 1)$ corresponds to the five largest observed this stress extended. These result from extensive shocks when moving the vehicle in five concrete bumps. A total of 17.7 % of the damage area of the figure reflects the severity of the extended amplitude whose average is positive. They reflect the effect of compression after passing on concrete bumps.

Contributions and Impact of a Statistical Modeling for Random Loading in the Calculation of Lifetime

Principle of Damage Calculating

Data around which theoretical models of probability density are of three kinds (part 1):

- The amplitudes grouped into classes.
- Extreme amplitudes.
- Envelope of the stress.

Thus, three models of calculation will be presented in the following paragraphs. The evolution of damage is always calculated from the model Miner. We write an element of damage by fatigue dD is due to a stress element dn. Under the law of Miner

$$dD = \frac{dn}{N(S)} \tag{76}$$

with dn number of amplitudes solicitation studied at the level between S and $S + ds$.

- For a given duration T,

$$dn = N_T \times f_S(s)\, ds,$$

  with N_T the total number of stresses and $f_S(s)$ probability density of the time stress whose level is equal to S.
- To stress measured with a time step $\Delta t = 1/f_e$ (f_e sampling frequency), the total number of stresses is equal to $N_T = f_e \times \mathrm{T}$. Thus, the global damage is the sum of the partial damage for all values f S:

$$D = N_T \times \int_{\Delta} \frac{f_S(s)}{N(S)} \times ds \tag{77}$$

  with $\Delta =$ domain of definition of S.
- Where the Wöhler is regarded as the model Basquin:

  In this case, ($NS^b = C$, C is a constant depending on the level of stress), Eq. (76) becomes:

$$D = \frac{N_T}{C} \times \int_{\Delta} s^b \times f_S(s) \times ds \tag{78}$$

  If we set

$$u = \frac{s}{\sqrt{V(S)}}$$

  with $V(S)$ variance S. Relation Eq. (78) is written:

$$D = [V(S)]^{b/2} \frac{N_T}{C} \times \int_{\Delta} u^b \times f_U(u) \times du \tag{79}$$

Table 5 Calculation of damage according to the Pearson system (see Fig. 36)

Laws of probability[a]	Damage D	
Beta 1 (Fig. 36)	$D = [V(S)]^{b/2} \frac{N_T}{C} \frac{\gamma(p+q)\gamma(b+p)}{\gamma(p)\gamma(b+p+q)}$	(80)
Beta 2 (Fig. 36)	$D = [V(S)]^{b/2} \frac{N_T}{C} \frac{\gamma(q-b)\gamma(b+p)}{\gamma(p)\gamma(q)}$	(81)
Log-Normal (Fig. 36)	$D = [V(S)]^{b/2} \frac{N_T}{C} \exp\left(bm + \frac{b^2 ff^2}{2}\right)$	(82)
Gamma (Fig. 36)	$D = [V(S)]^{b/a} \frac{N_T}{C} \frac{\gamma(b+p)}{a^b \gamma(p)}$	(83)
Weibull (Fig. 36)	$D = [V(S)]^{b/2} \frac{N_T}{C} \eta^b \gamma\left(1 + \frac{b}{\beta}\right)$	(84)
Normale (Fig. 36)	$D = [V(S)]^{b/2} \frac{N_T}{C\sqrt{2\pi}} 2^{\frac{b}{2}-1} \gamma\left(\frac{b+1}{2}\right)$	(85)

[a]See also Appendix 1

Thus, the damage is D calculated for each amplitude family around which a probabilistic modeling is proposed (Sect. 1). Firstly, the calculation can be done according to the system of Pearson (Beta 1 law, Beta 2 law and Log-Normal law, Gamma Law and Weibull law, Normal (or Gaussian) law. Calculation can also be done using either the law of Gram-Charlier–Edgeworth or the law of the envelope (or Rice).

Damage Calculating on the Basis of Laws Obtained by Pearson System

Table 5 gives the result of the relationship Eq. (79), obtained by the Pearson system for each probability law or each equivalent law. The laws of probability so that their parameters are given in Appendix 1.

Figure 36 shows the influence of parameters that define the laws of probability on the global damage. It is clear that the damage D decreases with increasing exponent b because when b increases (for a given C), the lifetime increases with the model Basquin.

Damage Calculating on the Basis of the Gram-Charlier–Edgeworth Law

In this case, the calculation from Eq. (79) is performed with the probability density function expressed with Eq. (11). Equation (79) leads to the following Eq. (86):

$$D = [V(S)]^{b/2} \frac{N_T}{C\sqrt{2\pi}} \left\{ \begin{array}{l} \gamma\left(\frac{(1+b)}{2}\right)\left(1+(-1)^b\right) \cdot \left\{ \begin{array}{l} 2^{\left(\frac{b-1}{2}\right)} + 2^{\left(\frac{b+1}{2}\right)} \\ \times \left[\left(\frac{k_3^2 b}{18}\right) + \left(\frac{k_3^2 b^2}{14}\right) + \left(\frac{k_4 b^2}{48}\right) - \left(\frac{k_4 b + k_3^2 b^2}{24}\right)\right] \end{array} \right\} \\ + \gamma\left(\frac{b}{2}+1\right) 2^{\frac{b}{2}} k_3 \left(\frac{b-1}{6}\right)\left(1-(-1)^b\right) \end{array} \right\} \tag{86}$$

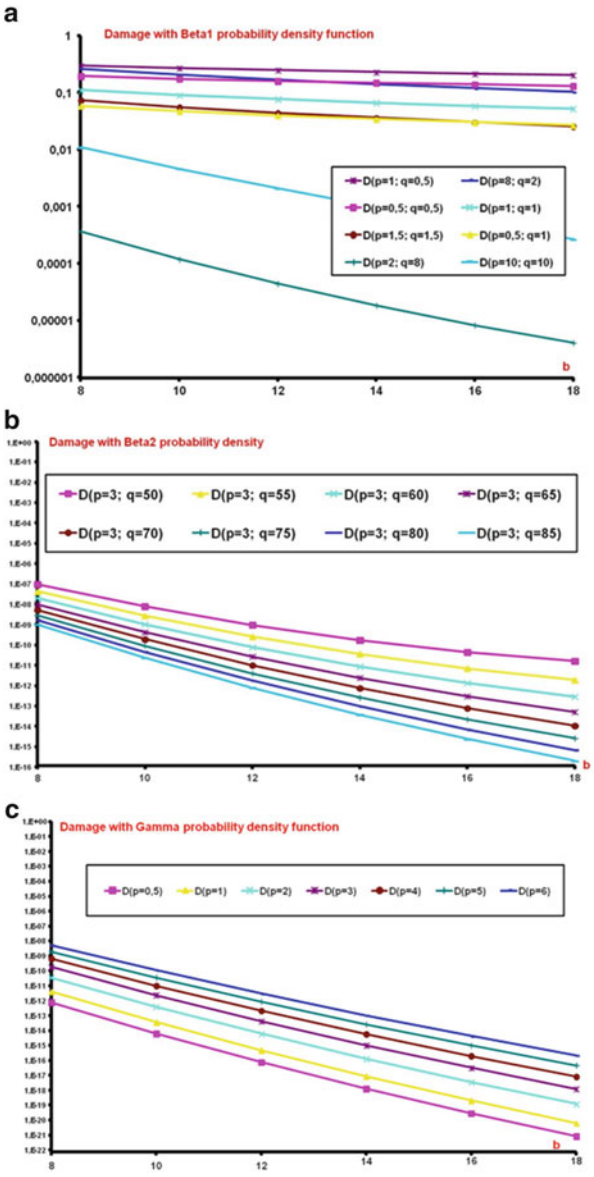

Fig. 36 Evolution of damage depending on the settings of each probability distribution. (**a**) Damage with Beta 1, (**b**) damage with Beta 2, (**c**) damage with gamma, (**d**) damage with Weibull, (**e**) damage with Log Normal, (**f**) damage with Gauss

Figure 37 shows the evolution of the damage function of b, the skewness β_1, and β_2 kurtosis of the stress distribution. All curves decrease with the increase of the parameter b. For a given β_1 parameter when kurtosis β_2 increases, that is to say, the dispersion of the stress distribution and damage increases, when the skewness ratio increases, the damage also.

Fig. 36 (continued)

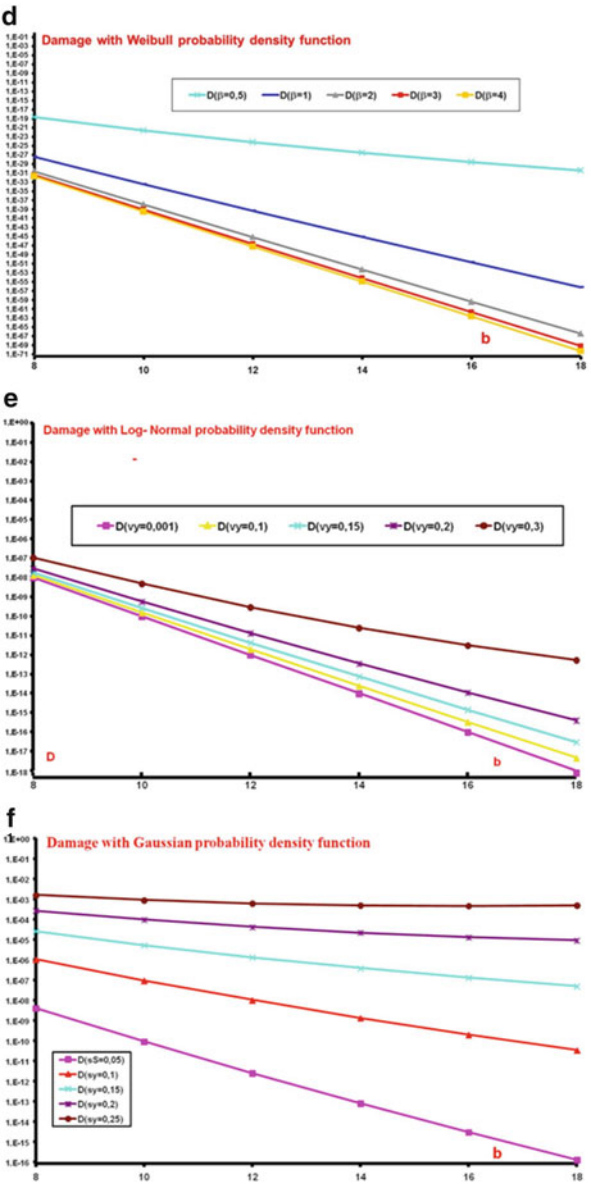

Damage Calculating on the Basis of the Rice Law on the Envelope

The presented model of the envelope in Sect. 2.4 and Appendix 5 relates extrem amplitudes, so the total number of stresses is equal to the number N_T extrem amplitudes N_e. In this case, the damage is determined by the relationship

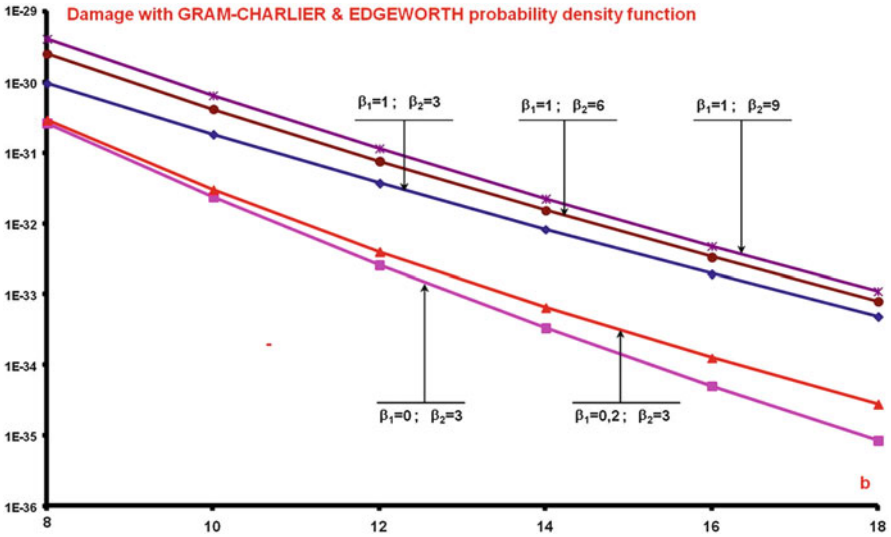

Fig. 37 Evolution of damage according to the law of Gram-Charlier–Edgeworth

Table 6 Calculation of damage to individual cases of irregularity factor I

$I = 0$ (stress broadband)		$I = 1$ (stress narrowband)	
$D = [V(S)]^{\frac{b+1}{2}} \frac{N_e}{C} \frac{2^{\frac{b}{2}-1}\gamma\left(\frac{b+1}{2}\right)}{\sqrt{\pi}}$	(88)	$D = [V(S)]^{\frac{b+1}{2}} \frac{N_e}{C} 2^{\frac{b}{2}-1}\gamma\left(\frac{b}{2}+1\right)$	(89)

$$D \approx \frac{[V(S)]^{\frac{b+1}{2}} N_e}{C} \left\{ \begin{array}{l} \frac{2^{\frac{b}{2}-1}\left(1-I^2\right)^{\frac{b}{2}+1}\gamma\left(\frac{b+1}{2}\right)}{\sqrt{\pi}} + 2^{\frac{b}{2}-1} I \gamma\left(\frac{b}{2}+1\right) \\ + \frac{2^{\frac{b+1}{2}} I^3}{\left(1-I^2\right)\sqrt{(b+2)\pi}} \Phi\left(\frac{2I^2}{1-I^2}; 1; [b+2]\right) \end{array} \right\} \quad (87)$$

With $\Phi\ (x, 1, [b+2])$ is the cumulative probability function of Fischer–Snedecor of x in the degrees of freedom with one and the integer part of $(b+2)$.

Note $\Phi(0, 1, [b+2]) = 1$ and $\Phi(\infty, 1, [b+2]) = 0$. The results for the particular case of irregularity factor I are presented in Table 6:

The damage curves (Fig. 38) decrease as the parameter b is increased (slopes substantially equal to the slopes Fig. 37). When the irregularity factor changes from 0 (broadband) to a value of 1 (narrowband), damage increases. This effect is due to the increased number of cycles with a narrowband signal.

Applications (Brozzetti and Chabrolin 1986b)

Fatigue strength of a node type T "jacket" of an "offshore" structure must be checked. Available records concerning the height of the waves beat structure; values are based on the frequency of occurrence (Table 7). These records are related to a reference time of 1 year.

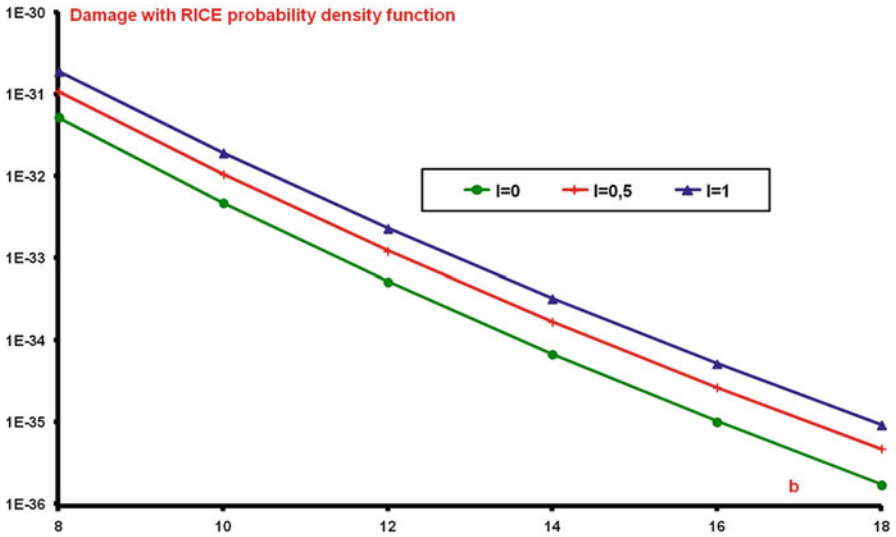

Fig. 38 Evolution of damage according to the law of the envelope of Rice

Table 7 Frequency of occurrence of solicitation for a T structure

No.	Wave height H (m)	Stress sizing $\Delta\sigma$	Annual number of waves $= n_i$
1	0	0	4,482,356
2	1.52	6.45	2,014,741
3	3.05	14.87	759,383
4	4.57	24.15	281,009
5	6.10	34.16	104,059
6	7.62	44.61	38,765
7	9.14	55.49	14,558
8	10.67	66.81	5,516
9	12.19	78.39	2,108
10	13.72	90.34	812
11	15.24	102.48	314
12	16.76	114.87	122
13	18.29	127.56	47
14	19.81	140.39	18
15	21.34	153.50	7
16	22.86	166.71	3
17	24.38	180.00	1
18	25.91	193.74	...

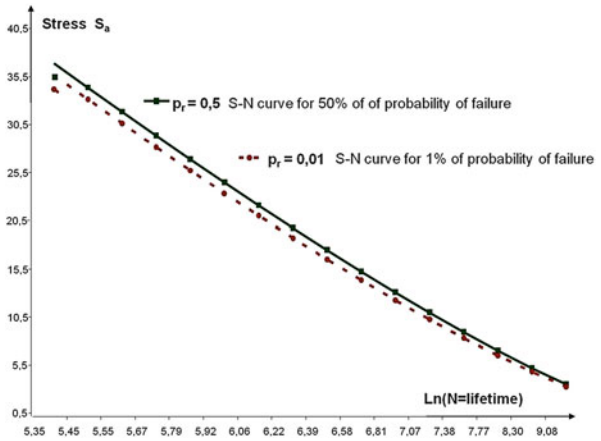

Fig. 39 Endurance curve (for T type node jacket) of an offshore structure

At each of these wave heights, the calculation of the structure leads to a stress on the design of the T node ($\Delta\sigma$, in MPa, Table 7). This constraint sizing takes into account a coefficient of stress concentration T node considered.

Fatigue curve at 50 % of the considered node failures is given by the expression (Basquin deviation) as follows:

$$N\Delta\sigma^{10} = 10^{10} \quad \text{or} \quad \log(N) = -3\log(\Delta\sigma) + 10 \tag{90}$$

Fatigue curve 1 % failure is as follows: $N\Delta\sigma^{2.9} = 10^{9.8}$. These curves are presented in Fig. 39.

Calculation of cumulative damage to the node as well as its lifetime can be made using the methods presented in the previous sections.

Calculation of Damage and Lifetime According to the Classical Method

Table 8 presents the calculation of cumulative damage by applying Miner's rule ("Calculation of fatigue damage, of damage accumulation and of lifetime" and "Introductory examples" in Appendix E). The accumulated damage of the fatigue curve with 50 % of failures provides a value $D_{(0,5)} = \Sigma(n_i/N_i) = 0.0147$ and the lifetime of the node $= 1/D = 68$ years. The calculation with the fatigue curve gives 1 % damage $D_{(0,01)} = 0.0193$ so a minimum lifetime of 52 years.

This approach to calculation is based on the observed numbers (n_i) and the lifetime limit estimated (N_i) for each level of the stress concerned. The statistical nature of the distribution of staff (or the probability amplitudes of the stress studied) is not taken into account. Moreover, this calculation of the global lifetime of endurance depends on the model given in Eq. (90).

Table 8 Damage and lifetime for a T structure

No	Stress (MPa)	Number of waves of height H (m)	N_i	n/N_i ($\times 10^{-4}$)
1	3, 225	2, 467, 615	42, 112, 482, 458	0.5860
2	10, 660	1, 255, 358	1, 166, 080, 106	10.7656
3	19, 510	478, 374	190, 207, 743	25.1501
4	29, 155	176, 950	56, 998, 163	31.0449
5	39, 385	65, 294	23, 121, 045	28.2401
6	50, 050	24, 207	11, 266, 467	21.4859
7	61, 150	9, 042	6, 177, 470	14.6371
8	72, 600	3, 408	3, 691, 392	9.2323
9	84, 365	1, 296	2, 352, 410	5.5092
10	96, 410	498	1, 576, 281	3.1593
11	108, 675	192	1, 100, 553	1.7446
12	121, 215	75	793, 105	0.9456
13	133, 975	29	587, 393	0.4937
14	146, 945	11	445, 180	0.2471
15	160, 105	4	344, 180	0.1162
16	173, 355	2	271, 138	0.0738
17	186, 870	1	216, 462	0.0462
Sum				0.0153

Calculation of Damage and Lifetime by Statistical Modeling

The process of calculation, in this paragraph, incorporates the statistical nature of the distribution of staff (or the probability amplitudes of the stress studied) and uses the same model of endurance expressed by Eq. (90). In this case, the damage is assessed from the following four elements:

- Law of distribution of wave heights in the long term
  In this example, distribution of wave heights corresponds to a Weibull law:

$$H = H_0 + p_{\text{cte}} \log(n). \tag{91}$$

  With H_0 is the maximum wave height recorded in the reference period (within 1 year); n is the number of wave heights greater than H_0, p_{cte} is a constant.
- Damage law (or curve of fatigue or S–N curve)

$$\text{Let}: \quad N\Delta\sigma^b = C, \quad \text{let}: N = C\Delta\sigma^{-b} \,(\text{same Eq. (90)}) \tag{92}$$

  With $b =$ slope of the S–N curve, $N =$ number of cycles associated with the variation of the stress sizing $\Delta\sigma$, $\Delta\sigma$ extent of stress variation in the node in T of the structure.

- Relationship between wave height H to the stress variation $\Delta\sigma$

  The stress variation $\Delta\sigma$ is laid as:

$$\Delta\sigma = \alpha.H^{\beta} \tag{93}$$

  with α and β two coefficients that are obtainable by smoothing spots $(\Delta\sigma, H)$.

  If the value of $\Delta\sigma$ given by the expression Eq. (93) in Eq. (92) is postponed, we obtain:

$$N = C\alpha.\left(H^{\beta}\right)^{-b} \tag{94}$$

  Transformation of expression Eq. (91) gives:

$$n = n_0.\exp\left(2.3026H/p_{\text{cte}}\right) \tag{95}$$

  With $n_0 = 10^{-H_0/p_{\text{cte}}}$.

- Rule of damage cumulation

$$\Delta D = dn/N \tag{96}$$

  Thus,

$$dn = \left(2.3026/p_{\text{cte}}\right) n_0 \exp\left(2.3026H/p_{\text{cte}}\right)\ dH \tag{97}$$

  We obtain:

$$\Delta D = dn/N = \alpha^b \left(2.3026/C.p_{\text{cte}}\right) n_0 \exp\left(2.3026H/p_{\text{cte}}\right) H^{b\beta}\ dH \tag{98}$$

  Let:

$$D = \frac{2.3026 n_0 \alpha^b}{C.p_{\text{cte}}} \int_0^{\infty} \exp\left(\frac{2.3026\ H}{p_{\text{cte}}}\right) H^{b\beta}\ dH \tag{99}$$

  We recall that : $\int_0^{\infty} t^u \exp\left(-vt^w\right) dt = \frac{\gamma[(u+1)/w]}{wv^{(u+1)/w}}$; $\gamma(t)$ is the gamma function (see Eq. (28)) with $u = \beta bv = 2.3026/p_{\text{cte}}$ and $w = 1$, we obtain

$$D = \frac{2.3026 n_0 \alpha^{-b}}{C.p_{\text{cte}}} \frac{\gamma\left(\beta b + 1\right)}{\left(\frac{2.3026}{p_{\text{cte}}}\right)^{(\beta b+1)}} \tag{100}$$

Example 3 From the data in Table 7, we obtain by smoothing:

$$H = 6.1 + 0.913\log(n)\quad (H \text{ in meters}) \qquad \Delta\sigma = 3.9H^{1.2}.$$

Table 9 Summary of results for structure T application

Summary of results for structure T application	Traditional approach	Statistical modeling
Material distribution	Yes	Yes
Load distribution	No	No
50 % failure probability (reliability 0.5)	LT = 68 years	LT = 73 years
1 % failure probability (reliability 0.99)	LT = 52 years	LT = 49 years

Let: $\alpha = 3.9$; $\beta = 1.2$; $b = 3$; $p_{\text{cte}} = 0/913$; $C = 10^{10}$; $H_0 = 6.1$; $n_0 = 10^{6.1/0.913}$.

Hence: $\gamma(b\beta + 1) = \gamma(4{,}6) = 13.38$; $\alpha^b = 59.32$; $2.3026 n_0 = 11{,}053{,}226$; $p_{\text{cte}}.C = 0.913 \times 10^{10}$.

Thus, damage: $D = 0.0137$.

So the lifetime is $1/D = 73$ years.

With the model of endurance to 1 % failure ($N\Delta\sigma^{2.9} = 10^{9.8}$), the lifetime is equal to 49 years.

In summary for this application (see Table 9), the transition from a traditional approach to statistical modeling provides a better prediction of behavior (7 % saving). It is also noted that the increase of reliability of from 0.5 to 0.99 decreases calculated lifetime to about 28 %.

Calculation of Damage and Lifetime on the Basis of Power Spectral Density (Lalanne 1999b)

A system or a mechanical component has a response to applied stresses (PSD). This response can be either measured on a prototype under tested qualification, either calculated from a global mechanical model.

The expression Eq. (79) shows that the damage depends on the variance of the amplitudes of the stress. The relation Eq. (46) gives the expression for the variance of a random stress according to its PSD. It must be previously represented by several levels (G_i). In this case, the relation Eq. (79) is then expressed as follows:

$$D = \frac{N_T}{C}[V(S)]^{b/2}\int_{\Delta} u^b f_U(u)\,du = \frac{N_T}{C}\cdot\left[\frac{\frac{\pi}{4\xi}\sum_{i=1}^{n} G_i\left[I_0(h_{i+1}) - I_0(h_i)\right]}{(2.\pi)^4 f_0^3}\right]^{b/2}\int_{\Delta} u^b f_U(u)\,du \tag{101}$$

- This expression is called "Fatigue Damage Spectrum" (Lalanne 1999b). The terms $\int_{\Delta} u^b f_U(u)\,du$ and $\frac{N_T}{C}$ are two multiplicative constants of the term expressed in the brackets of the expression Eq. (101). This term represents the evolution of the variance of the stress according to the frequencies.

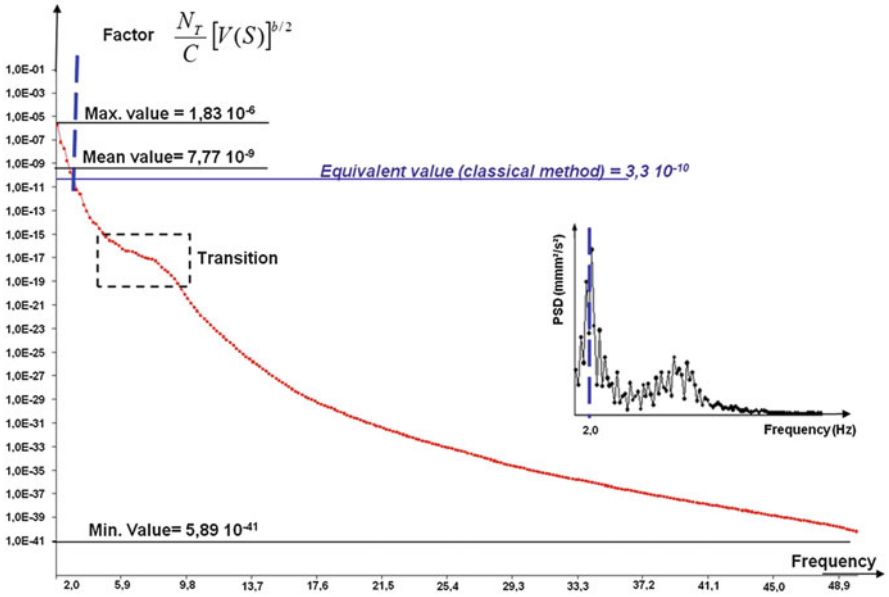

Fig. 40 Fatigue damage spectrum depending on the frequency

- Figure 40 shows the next term $\frac{N_T}{C}[V(S)]^{b/2}$ of the Fatigue Damage Spectrum on the stress shown in Fig. 10. This graph is obtained for $C = 10^7$ and $b = 12$, the value of b is given by (Lambert 1980) as an average value of the slope of the line for Basquin steels. The failure probability is 1 %. In Fig. 40, there is not a particular representative value to summarize the shape of the curve. However, an average value may be deducted, equal to 7.77×10^{-9} (the minimum is 5.89×10^{-41} and the maximum is 1.83×10^{-06}).
- The value of the term $\int_{\Delta} u^b f_U(u)\, du$ depends on the model probability density which is adopted for the stress studied. In the case of a Gaussian distribution, this sum is $\frac{2^{\frac{b}{2}}}{\sqrt{2\pi}}\gamma\left(\frac{b+1}{2}\right)$ (see relation Eq. (85)). The value here is equal to 18,425 (for $b = 12$). Thus, the average damage D_{av} is 1.43×10^{-4} (with a minimum damage equal to 1.09×10^{-36} D_{min} and D_{max} maximum damage equal to 3.37×10^{-2}). The lifetime (or the number of repetitions to failure $1/D_{\text{av}}$) is equal to 6,993.
- This calculation of the lifetime by the PSD as takes into account all the contributions of the stress on the frequency domain of stresses. The shape of the Fatigue Damage Spectrum is thus brought into relationship with the shape of the PSD (Power Spectral Density). The PSD of the stress studied (Fig. 13b) is outlined in Fig. 40. Thus, the almost flat spectrum observed in the fatigue damage in the area of transition nature (framed part in Fig. 40) is due to the

transition between the two major contributions observed on the PSD. These two are the two main modes, the stress observed studied.

- Note that the damage calculation by conventional method (described in "Calculation of fatigue damage, of damage accumulation and of lifetime" and "Introductory examples" in Appendix 5) gives damage $D_{\text{conventional}}$ equal to 6.05×10^{-6}. This level of damage is equivalent value $\frac{N_T}{C}[V(S)]^{b/2} = 3.3{\times}10^{-10}$, value that is located in the terminals and mini max damage (Fig. 40).

However, conventional method gives a value of damage to a single class of frequency (around 2 Hz) corresponding to the largest amplitudes of the PSD. Lifetime (or the number of repetitions before failure $1/D_{\text{conventional}}$) is then equal to 165,273 repetitions. The difference between the result of the lifetime by PSD and that obtained by the conventional method is now 95 %, results become very different.

Result obtained with Fatigue Damage Spectrum allows differentiation the role of each frequency band to obtain the damage. Damage results consequences of any stresses represented by the spectral density PSD. Damage obtained by this method takes into account all frequency levels that appear with their stress levels and their respective numbers.

Plan of Validation Tests

The different models presented to assess the damage and the lifetime in real use conditions based on different types of analysis of stresses measured on a system or a mechanical component. These models also allow defining test environments that must cause similar effects to those observed in the actual conditions of use.

- The experimental means perfect more and more to reproduce in laboratory the stresses recorded in real conditions of use. These types of tests are designed to validate models of mechanical calculation and are not intended to validate the lifetime estimated by the models presented earlier. Such validation would require too much time. Indeed, the need to reduce more and more the validation period of a product required to do as much as possible, test duration shorter and shorter and more severe than the stress level observed in the actual conditions of use. Naturally, these severe tests shall show equivalent to those observed in real use conditions consequences.

  Damage is an equivalence indicator.
- Figure 41 illustrates the principle of equivalent damage. In the case of alternating stresses and with a material whose curve of resistance to fatigue (Wöhler curve) is known, the limit lifetime is expressed in terms of alternating stress of solicitation. If we assume that the actual conditions of use are summarized in n_{real} repetitions of a sinusoidal stress ($S_a = S_{\text{real}}$) which is N_{real} the limit lifetime in these conditions of use ($n_{\text{real}} < N_{\text{real}}$). In this case (according to Miner), damage under real conditions of use is: $d_{\text{real}} = \frac{n_{\text{real}}}{N_{\text{real}}}$.

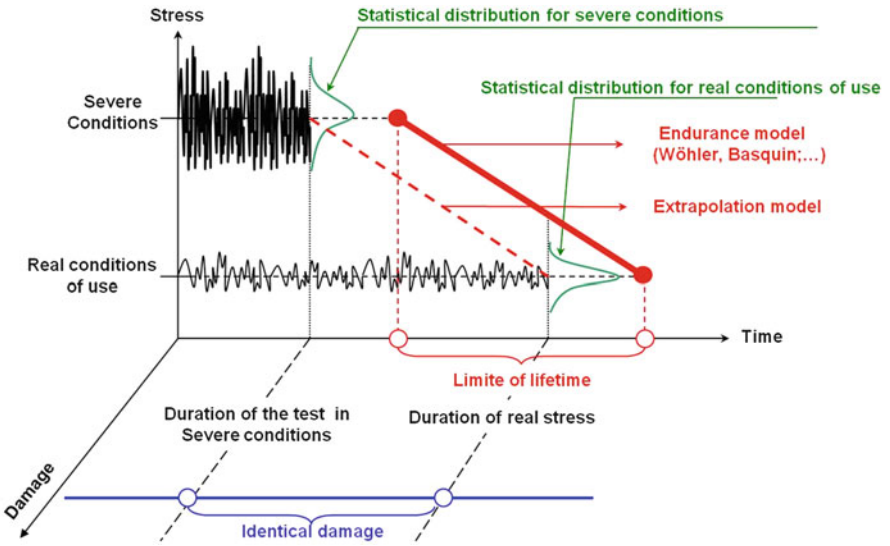

Fig. 41 Schema of the principle of equivalent damage

- Conducting a test in more severe conditions and leads to the same level of damage d_{real} is to define the number of times (n_{severe}) to be repeated a sinusoidal stress ($S_{\text{a}}^{'} = S_{\text{severe}}$) so that the damage d_{severe} is equal to d_{real}.
- For a mechanical component, the level ($S_{\text{a}}^{'} = S_{\text{severe}}$) is determined depending on the material which constitutes the studied and knowledge about limits behavior component. The equivalence between damage ($d_{\text{severe}} = d_{\text{real}}$) leads to the calculation of n_{severe}. As follows:

$$n_{\text{severe}} = \frac{N_{\text{severe}}}{N_{\text{real}}} n_{\text{real}} \tag{102}$$

  According to the model Basquin $N = CS^{-b}$, then

$$n_{\text{severe}} = \left(\frac{S_{\text{severe}}}{S_{\text{real}}}\right)^{-b} n_{\text{real}} \tag{103}$$

  Figure 42 illustrates the process of calculating the number of cycles required to produce, under severe conditions, damage equivalent to that observed under actual use conditions.
- A detailed analysis of behavior in endurance (long period) should help define tests (short term) to perform in laboratory or on simulation bench. In this case, it is advisable to retain only the critical stresses. Two selection criteria are possible: take only the stresses that have contributed from a given percentage of the global damage or take the stresses whose amplitude alternating (S_{a}, Fig. 31b) is greater than the limit endurance.

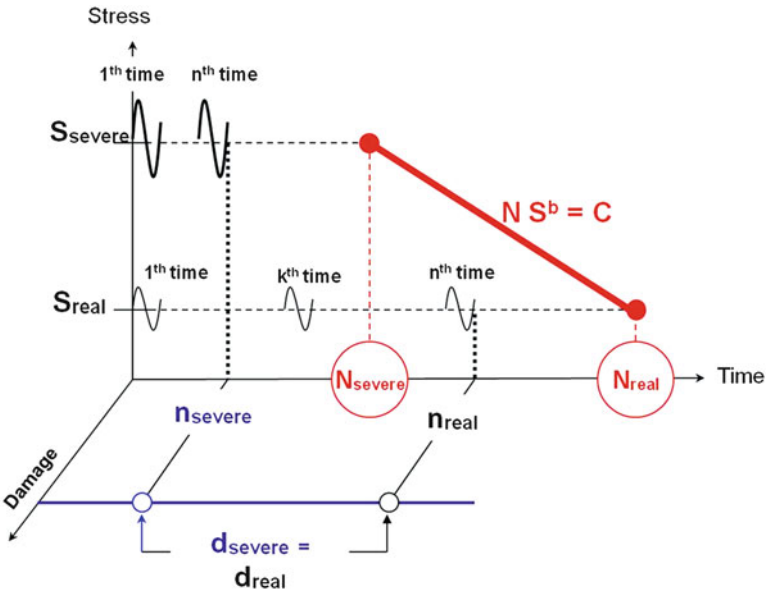

Fig. 42 Schema of the equivalent damage principle in the case of sinusoidal stresses

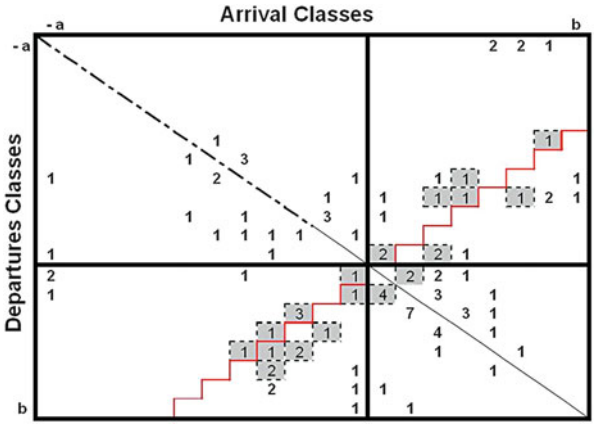

Fig. 43 Transition matrix of the stress with distinction parts of the alternating stresses which amplitude is less than the endurance limits (see Fig. 10)

For the examples presented in the following, this is the second criterion that is used.

– Figure 43 shows the transition matrix corresponding to the stress of Fig. 40 by specifying the boxes (with gray background) in which the associated alternating stress is below the endurance limit. If these stresses are not considered, the cumulative damage remaining 72 % of the global damage.

- The remaining part of the transition matrix can be used for testing in the laboratory. Of course, it is only the nonempty boxes of the matrix are taken into account.
- In the case of this stress, the information obtained by the extended-slope matrix (Fig. 21a) and the extreme-curves matrix (Fig. 21b) contributes to the definition of the dynamic sinusoidal stresses considered for each nonempty cell of the matrix of transition.
- In the top right quarter of the matrix linking extreme amplitudes and curvatures (Fig. 21b), there is five number which summarizes the five extreme amplitudes (negative) observed following the passage of the five concrete bumps. Based on the transition matrix (Fig. 10), these five amplitudes are the starting points of which types of stress do not have exactly the same end point. But the information provided by the extreme-curvature matrix confirms that these five amplitudes the frequency signature is identical.
- The frequency according to which occur these five amplitudes is calculated as:

$$\text{frequence} = \frac{1}{2\pi}\sqrt{\left|\frac{y''}{y}\right|} \tag{104}$$

with y'' is the second derivative of the signal y of load plotted against time.

- This relationship can also calculate all the frequencies of stresses that must be applied during laboratory tests. These are the quarters on up and right and down left of the extremes-curvatures matrix which are favored because they plot stresses whose sign of the amplitude of departure is different from the amplitude of arrival, reflecting extent of high amplitude. The quarters up left and down right plot intermediate fluctuations which are not important as long as they remain concentrated around the center of the matrix.

- The transition matrix of Fig. 44a shows a stress history near a fillet weld on a transport vehicle chassis (Kouta et al. 2002) in an actual path of usage of 464 km. Figure 44b shows this same matrix in the form of Iso-curves (or level curves). This second representation gives iso-level curves of log of numbers, for an easier viewing. In red (center of the butterfly), there are more effective but they are the least damaging. By against in blue, the lowest numbers are shown but the most damaging. For this case of loading, figure is symmetrical with respect to the first diagonal, and is offset slightly downwardly. Note also the existence of two small separate areas from the main figure.

  - A first failure on the ground was observed on this path of 464 km after 1E + 06 km (2,155 rehearsals). Endurance characteristics of the material (Wöhler curve) were determined through laboratory tests on this type of component. The calculation of lifetime through the approach presented earlier ("Calculation of fatigue damage, of damage accumulation and of lifetime" and "Introductory examples" in Appendix 5) leads to a calculated lifetime of 1.2E + 06 km, which was satisfactory.

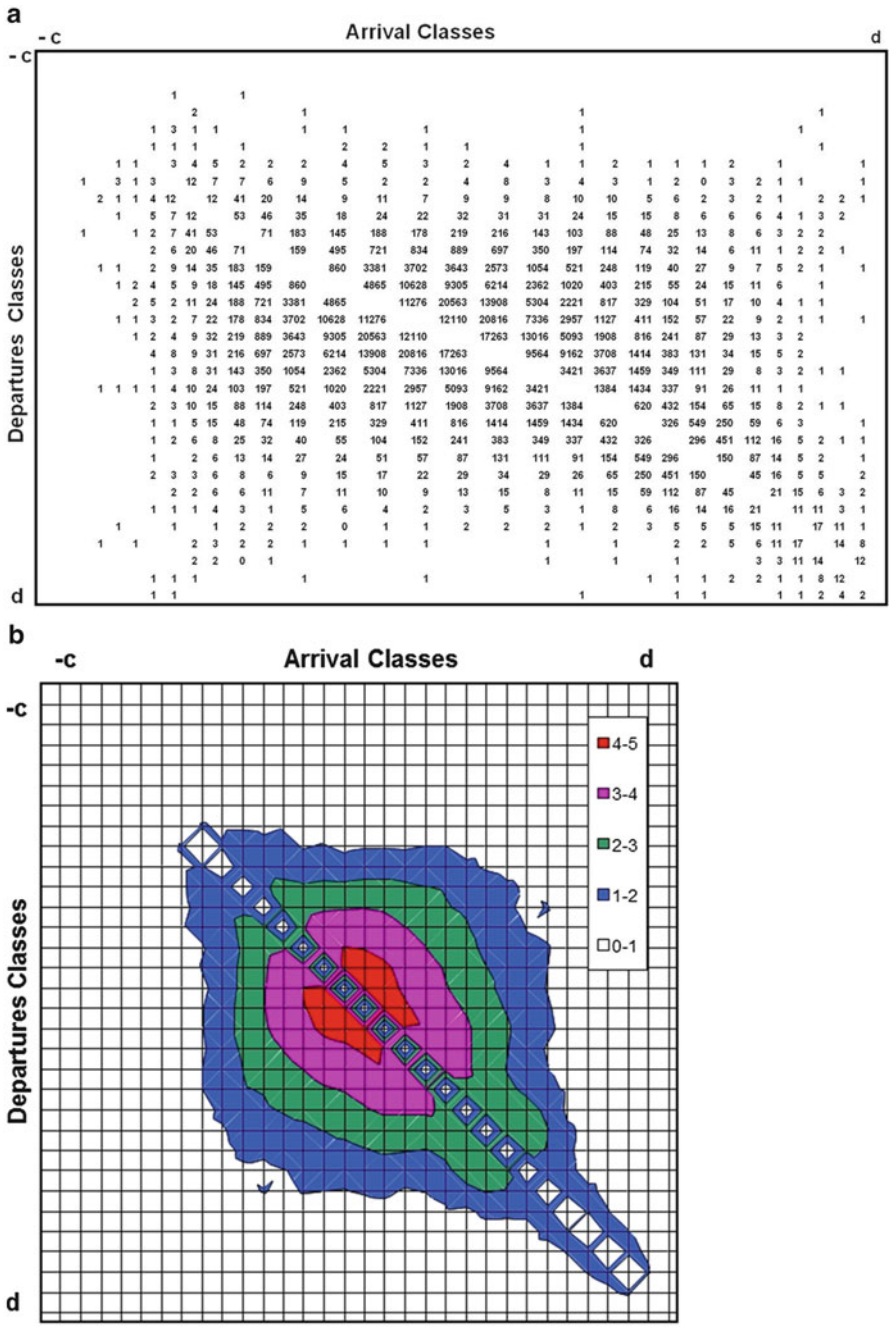

Fig. 44 Two representations (**a** stress history and **b** iso-curves) of a transition matrix for a fillet weld of the bogie chassis (according to (Kouta et al. 2002))

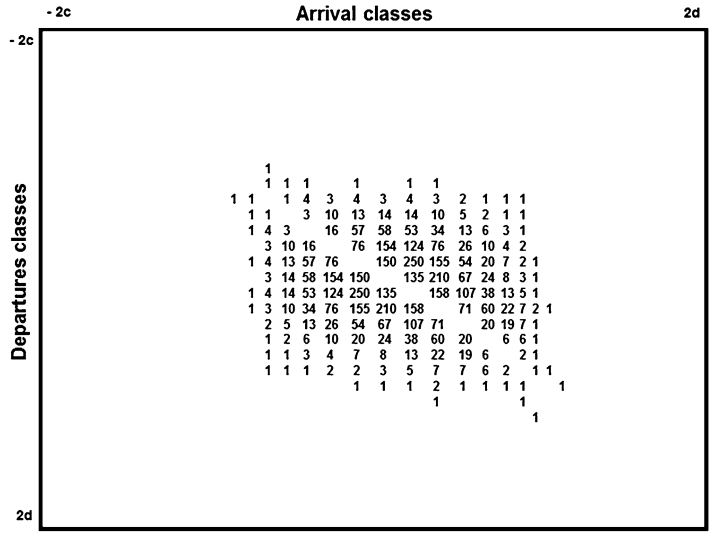

Fig. 45 Transition matrix corresponding to an endurance test obtained with a ratio of severity equal to 2 from the matrix in Fig. 43 (Matrix obtained under the rule of equivalent damage, see Eq. (102))

- The conditions of an endurance test of short-term representative of the actual damage were defined from Eq. (103). Figure 45 shows the transition matrix corresponding to an endurance test which is obtained with a ratio of severity equal to 2 $\{(S_{\text{severe}}/S_{\text{real}}) = 2$, amplitude -2c, $+2$d$\}$. This matrix provides the same damage as observed by considering the matrix in Fig. 44 but with a test duration which corresponds to a distance of 5 km with a rehearsal. Thus, this new matrix can be used to achieve a short-term endurance test in laboratory whose consequences (analysis of cracks, probable failure, etc.) are representative of a real long-term use.

Conclusion

The approach presented in three parts was motivated by the challenges of quality requirements for mechanical systems and components. And more specifically, lifetime and reliability (probability of no break) are two main features. All of the tools can be naturally applied to all cases of random stresses in mechanical. Engineers of design and development in mechanical have to know in detail:

- Actual conditions of use from users' behaviors.
- Actual conditions of use from users' behaviors.
- Behaviors (or responses) of studied systems.
- Models of material degradation.

Thus achieve the provision of values lifetime is not an insurmountable task. However, numerical results should always be viewed and analyzed the same time as the assumptions that lead to their obtaining.

Different approaches for calculating lifetime were presented as well as intermediate hypotheses required to calculate:

- Approach with statistical modeling ("Contributions and Impact of a Statistical Modelling for Random Loading in the Calculation of Lifetime" section in Appendix 5) can now relay conventional approach ("Calculation of Fatigue Damage, of Damage Accumulation and of Lifetime" and "Introductory Examples" sections in Appendix 5) traditionally used in design departments. This approach with statistical modeling provides a global indicator of damage, lifetime, and reliability which remains easy to obtain while having improved the quality of behavior prediction.
- Approach Fatigue Damage Spectrum with the use of the PSD is however in conjunction with the actual conditions of use of mechanical systems and components. Fatigue Damage Spectrum whose the method of obtaining has been developed in "Calculation of Damage and Lifetime on the Basis of Power Spectral Density (Lalanne 1999b)" in Appendix 5, allows to connect lifetime (or damage) of a mechanical component with dynamic characteristics of stresses sustained by the material. The use of PSD in this calculation allows taking into account the dynamic behavior of the system which belongs to the mechanical component studied. In addition, this approach allows taking into account the nature of the statistical distribution of the solicitation.
- Validation of predictive calculations in systems and mechanical components design also calls for the establishment of specific test procedures. Naturally, market pressure requires test times which are compatible with the terms of product development. In general, these periods have nothing to do with expected lifetime in service. The obtained results allow constructing simple environments of bench testing of similar severity to that observed in tests of endurance.

References

Arquès P-Y, Thirion-Moreau N, Moreau E (2000) Les représentations temps-fréquence en traitement du signal [R 308]. Base documentaire « Mesures et tests électroniques ». (*)

Banvillet A (2001) Prévision de durée de vie en fatigue multiaxiale sous chargements réels : vers des essais accélérés. Thèse de doctorat no 2001-17, ENSAM Bordeaux, France (274 pp)

Bedard S (2000) Comportement des structures de signalisation aérienne en aluminium soumises à des sollicitations cycliques. Mémoire de maîtrise ès sciences appliquées, École polytechnique de Montréal, 0-612-60885-9

Borello G (2006) Analyse statistique énergétique SEA [R 6 215]. Base documentaire « Mesures mécaniques et dimensionnelles ». (*)

Brozzetti J, Chabrolin B (1986a) Méthodes de comptage des charges de fatigue. Revue Construction Métallique (1)

Brozzetti J, Chabrolin B (1986b) Méthodes de comptage des charges de fatigue. Revue Construction Métallique, no 1

Buxbaum O, Svenson O (1973) Zur Beschreibung von Betriebsbeanspruchungen mit hilfe statistischer Kenngrößen. ATZ Automobiltechnische Zeitschrift 75(6):208–215

Chang JB, Hudson CM (1981) Methods and models for predicting fatigue crack growth under random loadings. ASTM, STP 748, Philadelphia, PA

Chapouille P (1980) Fiabilité. Maintenabilité [T 4 300]. Bases documentaires « Conception et Production » et « Maintenance ». (*)

Charlier CVL (1914) Contributions to the mathematical theory of statistics. Arkio für Matematik (Astronomi och Fysik) 9(25):1–18

Clausen J, Hansson JSO, Nilsson F (2006) Generalizing the safety factor approach. Reliab Eng Syst Safety 91:964–973

Doob JL (1953) Stochastic process. Wiley, New York, 654 pp

Duprat D (1997) Fatigue et mécanique de la rupture des pièces en alliage léger [BM 5 052]. Base documentaire « Fonctions et composants mécaniques ». (*)

Edgeworth FY (1916) On the mathematical representation of statistical data. J Roy Stat Soc A, 79, Section I, pp 457–482; section II, pp 482–500; A, 80, section III, pp 65–83; section IV, pp 266–288; section V, pp 411–437 (1917)

Fatemi A, Yang L (1998) Cumulative fatigue damage and life prediction theories: a survey of the state of the art for homogeneous materials. Int J Fatigue 20(1):9–34

Fauchon J Probabilités et statistiques INSA-Lyon, cours polycopiés, 319 pp

Gregoire R (1981) La fatigue sous charge programmée, prise en compte des sollicitations de service dans les essais de simulation. Note technique du CETIM no 20, Senlis

Grubisic V (1994) Determination of load spectra for design and testing. Int J Vehicle Des 15(1/2):8–26

Guldberg S (1920) Applications des polynômes d'Hermite à un problème de statistique. In: Proceedings of the International Congress of mathematicians, Strasbourg, pp 552–560

Heuler P, Klätschke H (2005) Generation and use of standardized load spectra and load-time histories. Int J Fatigue 27:974–990

Jeffreys H (1961) Theory of probability, 3rd edn. Clarendon, Oxford

Johnson NL, Kotz S (1969) Distributions in statistics: continuous unvaried distributions—1. Houg. Mifflin Company, Boston, 300 pp

Kendall MG, Stuart A (1969) The advanced theory of statistics, vol 1. Charles Griffin and Company Limited, London, 439 pp

Klemenc J, Fajdiga M (2000) Description of statistical dependencies of parameters of random load states (dependency of random load parameters). Int J Fatigue 22:357–367

Kouta R (1994) Méthodes de corrélation par les sollicitations pour pistes d'essais de véhicules. Thèse de doctorat, Institut national des sciences appliquées de Lyon, no 94ISAL0096

Kouta R, Play D (1999) Correlation procedures for fatigue determination. Trans ASME J Mech Des 121:289–296

Kouta R, Play D (2006) Definition of correlations between automotive test environments through mechanical fatigue damage approaches. In: Proceedings of IME Part D: Journal of Automobile Engineering, vol 220, pp 1691–1709

Kouta R, Play D (2007a) Durée de vie d'un système mécanique—Analyse de chargements aléatoires. [BM 5 030]. (*)

Kouta R, Guingand M, Play D (2002) Design of welded structures working under random loading. In: Proceedings of the IMechE Part K: journal of multi-body dynamics, vol 216, no 2, pp 191–201

Lalanne C (1999a) Vibrations et chocs mécaniques—tome 4: Dommage par fatigue. Hermes Science Publications, Paris
Lalanne C (1999b) Vibrations et chocs mécaniques—tome 5: Élaboration des spécifications. Hermes Science Publications, Paris
Lallet P, Pineau M, Viet J-J (1995) Analyse des sollicitations de service et du comportement en fatigue du matériel ferroviaire de la SNCF. Revue générale des chemins de fer, Gauthier-Villars éditions, pp 19–29
Lambert RG (1980) Criteria for accelerated random vibration tests. Thèses. Proceedings of IES, pp 71–75
Lannoy A (2004) Introduction à la fiabilité des structures [SE 2 070]. Base documentaire « Sécurité et gestion des risques ». (*)
Leluan A (1992) Méthodes d'essais de fatigue et modèles d'endommagement pour les structures de véhicules ferroviaires. Revue générale des chemins de fer, Gauthier-Villars éditions, pp 21–27
Leybold HA, Neumann EC (1963) A study of fatigue life under random loading. Proc Am Soc Test Mater 63:717–734, Reprint no 70—B
Lieurade H.-P. (1980a) Les essais de fatigue sous sollicitations d'amplitude variable—La fatigue des matériaux et des structures. Collection université de Compiègne (éditeurs scientifiques Bathias C, Bailon JP). Les presses de l'Université de Montréal
Lieurade H-P (1980b) Estimation des caractéristiques de résistance et d'endurance en fatigue—La fatigue des matériaux et des structures. Collection université de Compiègne, Éditeurs scientifiques: Bathias C, Bailon JP Les presses de l'université de Montréal
Lu J (2002) Fatigue des alliages ferreux. Définitions et diagrammes [BM 5 042]. Base documentaire « Fonctions et composants mécaniques ». (*)
Max J (1989) Méthodes et techniques de traitement du signal et applications aux mesures physiques, vol 1 & 2, 4th edn. Masson, Paris
Olagnon M (1994) Practical computation of statistical properties of rain flow counts. Fatigue 16:306–314
Osgood CC (1982) Fatigue design. Pergamon, New York
Parzen E (1962) Stochastic process. Holdenday, San Francisco, 324 pp
Plusquellec J (1991) Vibrations [A 410]. Base documentaire « Physique - Chimie ». (*)
Pluvinage G, Sapunov VT (2006) Prévision statistique de la résistance, du fluage et de la résistance durable des matériaux de construction. ISBN: 2-85428-735-5, Cepadues éditions
Preumont A (1990) Vibrations aléatoires et analyse spectrale. Presses polytechniques et universitaires romandes, Lausanne, 343 pp
Rabbe P, Galtier A. (2000) Essais de fatigue. Partie I [M 4 170]. Base documentaire « Étude et propriétés des métaux ». (*)
Rabbe P, Lieurade H-P, Galtier A (2000a) Essais de fatigue. Partie 2 [M 4 171]. Base documentaire « Étude et propriétés des métaux ». (*)
Rabbe P, Lieurade HP, Galtier A (2000b) Essais de fatigue—Partie I. [M 4 170]. (*)
Rice SO (1944) Mathematical analysis of random noise. Bell Syst Tech J 23:282–332, 24:46–156 (1945)
Rice J.R., Beer F.P., Paris P.C. (1964) On the prediction of some random loading characteristics relevant to fatigue. In: Acoustical fatigue in aerospace structures: proceedings of the second international conference, Dayton, Ohio, avril 29 - mai, pp 121–144
Rychlik I (1996) Extremes, rain flow cycles and damage functional in continuous random processes. Stoch Processes Appl 63:97–116
Saporta G (1990) Probabilités. Analyse des données et statistiques. Éd. Technip, 495 pp
Savard M (2004) Étude de la sensibilité d'un pont routier aux effets dynamiques induits par la circulation routière. 11e colloque sur la progression de la recherche québécoise des ouvrages d'art, université Laval, Québec
Schütz W (1989) Standardized stress-time histories: an overview. In: Potter JM, Watanabe RT (eds) Development of fatigue loading spectra. American Society for Testing Materials, ASTM STP 1006, Philadelphia, PA, pp 3–16

Société française de métallurgie (Commission fatigue) (1981) Méthodes d'analyse et de simulation en laboratoire des sollicitations de service. Groupe de travail IV « Fatigue à programme », document de travail, Senlis

Ten Have A (1989) European approaches in standard spectrum development. In: Potter JM, Watanabe RT (eds) Development of fatigue loading spectra. ASTM STP 1006, Philadelphia, PA, pp 17–35

Tustin W (2001) Vibration and shock inputs identify some failure modes. In: Chan A, Englert J (eds) Accelerated stress testing handbook: guide for achieving quality products. IEEE, New York

Weber B (1999) Fatigue multiaxiale des structures industrielles sous chargement quelconque. Thèse de doctorat, INSA-Lyon, 99 ISAL0056

(*)In Technical editions of the engineer (French publications).